Predictors of personal exposure to air temperature in peri-urban India

Carles Milà[a], Ariadna Curto[a], Asya Dimitrova[a], V. Sreekanth[bc],

Sanjay Kinra[d], Julian D. Marshall[b], Cathryn Tonne[a*]

a. ISGlobal, Universitat Pompeu Fabra, CIBER Epidemiología y Salud Pública, Barcelona, Spain

b. Department of Civil and Environmental Engineering, University of Washington, Seattle, WA, USA

c. Center for Study of Science, Technology & Policy, Bengaluru 560 094, India

d. Department of Non-communicable Disease Epidemiology, London School of Hygiene and Tropical Medicine, London, UK

* Corresponding autor: Cathryn Tonne

cathryn.tonne@isglobal.org

ISGlobal, Universitat Pompeu Fabra, CIBER Epidemiología y Salud Pública, Doctor Aiguader 88, 08003 Barcelona, Spain

Abstract

Characterizing personal exposure to air temperature is critical to understanding exposure measurement error in epidemiologic studies using fixed-site exposure data and to identify strategies to protect public health. To date, no study evaluating personal air temperature in the general population has been conducted in a low-and-middle income country.

We used data from the CHAI study consisting of 50 adults monitored in up to six non-consecutive 24h sessions in peri-urban south India. We quantified the agreement and association between fixed-site ambient and personal air temperature, and identified predictors of personal air temperature based on housing assessment, self-reported, GPS, remote sensing, and wearable camera data.

Mean(SD) daytime (6am – 10pm) average personal air temperature was 31.2(2.6)ºC and mean nighttime (10pm - 6am) average temperature was 28.8(2.8)ºC. Agreement between average personal air and fixed-site ambient temperatures was limited, especially at night when personal air temperatures were underestimated by fixed-site temperatures (MBE=-5.6ºC). The proportion of average personal nighttime temperature variability explained by ambient fixed-site temperatures was moderate (R^2_{mar}=0.39); daytime associations were stronger for women (R^2_{mar}=0.51) than for men (R^2_{mar}=0.3). Other predictors of average nighttime personal air temperature included residential altitude, ceiling height, and household income. Predictors of average daytime personal air temperature included roof materials, GPS-tracked altitude, time working in agriculture (for women), and time travelling (for men). No biomass cooking, urban heat island, or greenspace effects were identified.

R^2_{mar} between ambient fixed-site and personal air temperature indicate that ambient fixed-site temperature is only a moderately useful proxy of personal air temperature in the context of peri-urban India. Our findings suggest that people living in houses at lower altitude, with lower ceiling height and asbestos roofing sheets might be more vulnerable to heat. We also identified households with higher income, women working in agriculture and men with long commutes as disproportionately exposed to high temperatures.

Keywords

Heat; GPS; remote sensing; wearable camera; greenspace; urban heat island.

Abbreviations (in order of appearance)

LMIC: Low-and-middle income country

GPS: Global Positioning System

CHAI: Cardiovascular Health effects of Air pollution in Telangana, India

APCAPS: Andhra Pradesh Children and Parents Study

ICC: Intraclass Correlation Coefficient

RMSE: Root Mean Square Error

UHI: Urban Heat Island

GVI: Green View Index

NDVI: Normalized Difference Vegetation Index

R^2_{mar}: Marginal R^2

AC: Air Conditioning

AM: Arithmetic mean

SD: Standard Deviation

MBE: Mean Bias Error

CI: Confidence Interval

1. Introduction

There is growing evidence of the health effects of thermal stress in low-and-middle income countries (LMICs) (Green et al., 2019). Studies in India have estimated significant associations between heat and increased mortality and morbidity (Fu et al., 2018; Salve et al., 2018), as well as decreased worker productivity (Venugopal et al., 2016). Yet, recent evidence has also revealed a larger contribution of moderately cold temperatures to mortality than moderately hot and extremely hot and cold temperatures, which can be partly explained by the higher frequency of moderately cold days in parts of India (Fu et al., 2018). Modifiers of temperature-mortality associations include physiological factors such as gender, age, and pre-existing chronic diseases and morbidities; but also potentially other factors that may relate to temperature exposure such as occupation and socio-economic status (Ingole et al., 2017; Son et al., 2019).

Personal monitoring of environmental exposures is increasingly feasible with low cost devices, with possibility of improved, individual-level exposure assessment in epidemiologic studies (Tonne et al., 2017a). While in air pollution epidemiology there is an increasing use of wearable sensors to measure personal exposure to air pollutants (Steinle et al., 2013), temperature epidemiology studies have predominantly relied on ambient (i.e., measuring the background, environmental air temperature away from local sources of heat) fixed-site temperature measurements (Gasparrini et al., 2015) or gridded modelled ambient temperatures (Fu et al., 2018) as proxies of personal exposure (i.e., the contact between an individual and air temperature at exposure surfaces of the skin and lungs). Exposure measurement error in population studies when using fixed-site or gridded estimates has not been well characterized, largely due to the general lack of data on personal air temperature (Kuras et al., 2017). Identifying predictors of personal exposure can inform potential risk prevention strategies needed to protect public health (Lioy, 2010). This issue is increasingly a priority as part of climate change adaptation strategies given that heat waves are expected to be longer, more frequent, and more severe (Murari et al., 2015) due to global warming (IPCC, 2014) by the second half of the century in India.

Most studies that have measured personal air temperature exposure are based on occupationally exposed individuals (Runkle et al., 2019; Sugg et al., 2019, 2018; Uejio et al., 2018; Xiang et al., 2014) and may therefore have limited generalisability to the general population. The few studies that have performed personal monitoring of temperature in the general population have been conducted in high-income countries (Basu and Samet, 2002; Bernhard et al., 2015; Brook et al., 2011; Kuras et al., 2015). Of these,

one study included residents of rural communities (Bernhard et al., 2015) and two considered factors other than ambient temperature that could affect personal exposure (e.g., household income, education, and occupation), and those factors were self-reported (Bernhard et al., 2015; Kuras et al., 2015). Although previous studies have used GPS derived location to investigate the influence of location and time-activity on personal temperature in occupationally exposed populations (Sugg et al., 2018), to our knowledge, no previous studies to date have evaluated how personal exposure to temperature is influenced by objectively-measured microenvironments derived from wearable cameras.

Here, we use a data-driven approach to identify predictors of personal air temperature in a sample of the general population in peri-urban south India. Our specific objectives were to 1) quantify the agreement and association between ambient fixed-site and personal air temperature exposure and 2) identify additional predictors of personal exposure to air temperature based on housing assessment, self-reported, GPS, remote sensing, and wearable camera data.

2. Materials and methods

2.1 Study population and monitoring sessions

We used data from the panel study of the Cardiovascular Health effects of Air pollution in Telangana, India (CHAI) project (Tonne et al., 2017b). CHAI was approved by the Ethics Committees of Parc de Salut Mar (Barcelona, Spain), the Indian Institute of Public Health-Hyderabad (Hyderabad, India), and the National Institute of Nutrition (Hyderabad, India). CHAI builds on the Andhra Pradesh Children and Parents Study (APCAPS) cohort (Kinra et al., 2014), which included 6,944 participants distributed in 28 villages in a peri-urban area south of the city of Hyderabad, India (**Figure S1**). CHAI added extensive ambient and personal air pollution monitoring in a random gender and village-stratified sample (n=401) of the APCAPS population. A random subsample of 60 CHAI participants was also included in the panel study, whose objective was to identify locations and activities with high particulate air pollution concentrations using ambient, GPS, wearable camera, and personal air pollution monitors (Milà et al., 2018) (**Figure 1**). The Köppen-Geiger climate classification (Beck et al., 2018) of the study area is tropical wet and dry, characterised by warm temperatures (coldest monthly air temperature above 18ºC) and a marked dry season.

Each panel participant was monitored in up to six 24 hour non-consecutive sessions within 6 monitoring rounds set up between May 2015 and February 2016 (1st: 2015-05-13 to 2015-06-21, n=63; 2nd: 2015-06-24 to 2015-07-26, n=52; 3rd: 2015-08-04 to 2015-09-09, n=40; 4th: 2015-09-09 to 2015-10-13, n=40; 5th: 2015-12-12 to 2016-01-04, n=39; 6th: 2016-01-07 to 2016-02-20, n=37). Sessions were distributed across the four seasons of the study area: summer (March-May), monsoon (June-August), post-monsoon (September-November), and winter (December-February). The start of the monitoring campaign in summer 2015 happened to coincide with a heat wave affecting Telangana and other Indian states (Liberto, 2015), during which monitoring was temporally suspended to avoid an additional burden and ensure the wellbeing of the study participants, who in many cases had outdoor occupations involving physical activity. Monitoring sessions were scheduled so as to minimize the impact on participant's daily routines; they typically started at 8am at the participant's residence and finished 24 hours thereafter at the same location. A trained technician was present at both times to install and remove the monitoring devices, give instructions to the participants, answer questions, and administer a post-monitoring questionnaire.

Participants were instructed to place the rucksack near them when not wearing it to minimise measurement error.

2.2 Data sources

2.2.1 Personal air temperature

Continuous personal air pollution monitoring was conducted using a RTI MicroPEM v3.2A monitor (MicroPEM, RTI International, Research Triangle Park, NC 27709, USA) attached to the strap of a rucksack (**Figure S2**). The device included a low-voltage, precision centigrade temperature sensor (P/N TMP-36GT9Z-ND, Analog Devices Inc., Norwood, MA, USA) that recorded ambient temperature every 30 seconds. The sensor was located in the sample flow stream, downstream of the filter. According to the manufacturer, the temperature range of the device was -40ºC to 100ºC; accuracy at 25ºC was ±3ºC. Upon deployment of the device, the initial temperature of the sensor was calibrated with ambient temperature (measured with HTC-1 LCD Digital Thermometer Hygrometer) using the MicroPEM Docking Station software (version 2.0). The same software was also used to download the data after monitoring. We computed 1-minute average temperature time series from the raw data (**Figure S3**).

We performed a 4-hour laboratory experiment with four MicroPEM units used in the CHAI panel, a heater (Selecta Incubat), and a calibrated high-precision (± 0.1ºC accuracy) thermohygrometer (Testo 635-2; used as reference) to evaluate the following for the MicroPEM temperature sensor: 1) agreement and reproducibility of measurements, 2) accuracy compared to the reference, and 3) responsiveness to temperature changes. Detailed description of the methods, materials, and results from the experiment is available in **Methods S1**. Briefly, we found that while agreement between MicroPEM temperature sensors was excellent (Intraclass Correlation Coefficient, ICC=1), their response time was slow, resulting in differences in air temperature compared to the reference (Root Mean Square Error, RMSE = 1.7-2.1ºC among the four MicroPEM units) with successive 5ºC temperature increments every 30 minutes.

2.2.2 Ambient air temperature

Hourly ambient temperature was recorded at a fixed-location site in the north of the study area (Digit THL, LabJack Corporation, Lakewood, CO 80227 USA) (**Figure S1**). Ambient monitoring started one month later than personal monitoring (June 2015); we therefore imputed data for May 2015 using temperature data from Hyderabad south airport located 16km away from the ambient north site (**Figure**

S1) following previously used methods for ambient fixed-site air pollution imputation in the CHAI project (Milà et al., 2018). Namely, we fitted a linear regression model to ambient north site temperature using airport temperature and hour categorical indicators as predictors. The model had an adjusted-R^2 of 0.94; we used this model to predict north site hourly temperature for May 2015.

2.2.3 Questionnaires and housing assessment

CHAI participants completed a baseline questionnaire containing information about time-invariant demographic (age, gender), socioeconomic (education, occupation) and household (income, assets) characteristics. Bedroom materials, dimensions, and number of windows were assessed by a trained technician. Furthermore, a post-monitoring questionnaire was administered at the end of each monitoring session. The questionnaire included a series of questions about total daily time spent in certain activities (e.g., cooking) and locations (e.g., travelling), as well as a diary of activities and locations with hourly slots.

2.2.4 GPS

Panel participants' longitude, latitude, and altitude were recorded every 30 seconds through a GPS device (Etrex 20; Garmin, Inc., **Figure S4**) participants carried in a secured backpack. The accuracy of the GPS in the study area was 4 meters; we inspected and cleaned the tracks to exclude points with abrupt changes of position (>1km) and cold starts (>50m from residence at the start of the session). The front door of all participants' households was geocoded by field workers. We identified points within the Hyderabad ring road (identified through aerial tracing of OpenStreetMap) to explore potential Urban Heat Island effects (UHI). We also applied a map-matching spatiotemporal clustering algorithm (Donaire-gonzalez et al., 2016; Sanchez et al., 2017) to the GPS tracks to identify locations visited during the monitoring. Detected clusters at a linear distance smaller than 10m from the participant's home were labelled as "home" whereas the rest of clusters were considered "places other than home". A point was considered to belong to a cluster if the distance in time and space was less than 10m/30min, respectively. The remaining points were classified as "trips".

2.2.5 Wearable camera

Panel participants carried a wearable camera (Autographer, OMG Life, Oxford, UK) that took photographs of the environment in front of the participant (180º approximately) every 35 seconds (**Figure**

S2). The battery life of the device was 10 hours; participants were instructed to turn off the device at night when light conditions were poor. Participants had the option to turn off the camera when they wanted privacy and at the end of each monitoring session they could review and delete images they did not want to be part of research data. The resulting photographs were annotated by two trained technicians according to a set of locations (e.g., outdoors), activities (e.g., eating), and objects (e.g., biomass stove) set a priori. As a result, each photograph was assigned a Boolean value as having/not having a given item. The annotation protocol and validation have been described in detail elsewhere (Salmon et al., 2018). We constructed 1min regular Boolean time series for each annotation from the photograph timestamps following previously published methods (Salmon et al., 2018).

For photographs annotated as "outdoors", we also derived a Green View Index (GVI) to identify the presence of greenspace. We used the open-source Treepedia GVI algorithm (MIT Senseable City Lab, n.d.) to detect the proportion of pixels in the photographs that corresponded to greenspace. This approach has been previously applied to Google Street View data (Li et al., 2015). Briefly, the procedure uses a normalisation of the red, green, and blue spectral image components, then employs an image segmentation algorithm to generate thematic images, and finally applies a series of rules to differentiate green vegetation features from the rest (Li et al., 2015; MIT Senseable City Lab, n.d.). An example of the GVI algorithm applied to a wearable camera photograph is shown in **Figure S5**.

2.2.6 Remote sensing

We downloaded two cloudless Sentinel 2A (multi-spectral instrument) level-1C (top of atmosphere) images from the Copernicus Open Access Hub (ESA, n.d.) for the study area. The selected images corresponded to the summer (2016-04-09) and post-monsoon (2016-11-25) seasons. We used the Sen2cor v.2.5.5 processor (Louis et al., 2016) to perform atmospheric correction and obtain level-2A bottom-of-atmosphere products. We derived Normalized Difference Vegetation Index (NDVI, (NIR-red)/(NIR+red)) at 10m spatial resolution (**Figure S6**) to identify spatial patterns of greenspace in the study area. We intersected NDVI (pure intersection and 100m buffer mean) with the GPS tracks and the geocoded households using the post-monsoon image for monitoring sessions conducted in monsoon and post-monsoon (wet seasons), and the summer image for winter and summer (dry seasons) (**Figure S6**).

2.3 Data management

There were 271 24h monitoring sessions corresponding to the 60 participants of the panel. We included 227 sessions (83%) corresponding to 50 participants in our analyses after excluding sessions with self-reported or accelerometer (in rucksack) detected non-compliance with wearing the equipment. Excluded male participants of the CHAI panel were younger than the included ones, while excluded women were less likely to work in agricultural-related occupations (Salmon et al., 2018). For nighttime analyses, 8 (3.5%) sessions were further excluded because the participant did activities other than sleeping at night, and another 12 (5.3%) were excluded because the participant reported not sleeping in the bedroom where room characteristics were recorded.

We integrated all sources of data to create three different datasets for analysis based on whether participants were sleeping and the time unit of analysis: 1) nighttime (10pm - 6am; one observation per session, n = 207), 2) daytime (6am – 10pm; one observation per session, n = 227), and 3) hourly daytime (6am – 10pm; one observation per hour within session, n = 2713). More than 90% of the panel participants self-reported sleeping between 10pm and 11pm while a 80% still slept from 5am to 6 am; percentages before and after this period were lower (56% sleeping between 9pm and 10pm, 25% sleeping between 6am and 7 am). The three datasets contained average personal temperatures corresponding to the time ranges of the dataset and average ambient fixed-site temperatures matching personal monitoring date and time spans; time-invariant participant and household characteristics and season were also available in all datasets. The nighttime dataset included NDVI and altitude at the geocoded household, while the daytime datasets included NDVI and altitude averages computed using the corresponding GPS tracks. Daytime datasets also contained daily/hourly time spent in different locations and activities according to the GPS algorithm, the diary and other self-reported activities, and wearable camera annotations; as well as average daily/hourly GVI.

2.4 Statistical analyses

We calculated univariate descriptive statistics of all the variables included in the analysis and computed a spearman correlation matrix for continuous predictors. We calculated the Intra-class Correlation Coefficient (ICC) for personal temperatures to infer the proportion of the exposure variability happening between participant. In order to describe and plot temporal patterns in exposure, we smoothed ambient fixed-site and personal temperature time series using generalized additive models with a smooth term (cyclic cubic splines, suitable for cyclic processes (Wood, 2006)) for the time of day. We stratified

daytime analyses by gender as previous results showed marked differences in mobility and time-activity patterns in this population (Sanchez et al., 2017). We investigated the agreement between average nighttime and daytime ambient fixed-site and personal temperature using Bland-Altman plots for repeated measures per participant (Bland and Altman, 2007). We evaluated the association between average nighttime and daytime ambient fixed-site and personal air temperature using linear mixed models with a random intercept per participant to account for the repeated measurements per participant. We used the marginal R^2 (R^2_{mar}), i.e., the proportion of variance explained by the fixed effects, as a measure of the strength of the association (Nakagawa and Schielzeth, 2013).

We identified predictors of nighttime, and gender-stratified daytime and hourly daytime average personal temperature exposure using the full datasets previously described. Within each dataset, we discarded predictors with little variability, i.e., if more than 90% of the observations had the same value (e.g., having air conditioning (AC), or time spent cooking for daytime in men). We examined missing data patterns in each dataset; the data source with the most missing entries was the wearable camera (18.1% missing in daytime dataset) followed by GPS indicators (8.8% missing in daytime dataset) (**Table S1**). We multiply imputed missing data using the method of the chained equations (van Buuren and Groothuis-Oudshoorn, 2011); assumptions, models, and details about the multiple imputation are given in **Methods S2**. In order to select the relevant exposure predictors, we used an automated stepwise procedure that was able to accommodate the repeated measures design, the multiply imputed data, and the temporal autocorrelation in hourly daytime models. A complete description of the procedure is given in **Methods S3**. We computed R^2_{mar} across the final models fitted in each of the imputed datasets.

Analyses were done in R v3.5.3 (R Core Team, 2019) using the following packages for data management and visualization (Grolemund and Wickham, 2011; Hijmans, 2019; Hunziker, 2017; Iannone, 2019; Pebesma, 2018; Salmon, 2017, 2016, 2013; Wickham, 2017, 2016), imputation (van Buuren and Groothuis-Oudshoorn, 2011), and modelling (Bates et al., 2015; Jaeger, 2017; Pinheiro et al., 2018; Wood, 2006). We used ArcGIS (v10.2.1), Spatialite (v4.1.1), and QGIS (v2.12.3 Lyon) to clean GPS data. GVI was computed using the Treepedia package (MIT Senseable City Lab, n.d.) in Python 3.6.4. Supplementary maps were done in QGIS (v2.18.1 Las Palmas).

3. Results

3.1 Characteristics of the study population and exposures

3.1.1 Time-invariant characteristics of the study population

Mean age of the study participants was 43.2 (standard deviation, SD 13.7) years; women were older than men and had lower literacy (**Table 1**). Most participants had manual occupations in the agriculture, construction, and other unskilled sectors. Only three participants reported having AC at home. The majority of participants lived in separate houses at a mean altitude of 570 meters above the sea level. The most prevalent material for bedroom walls was brick whereas roof and floor materials were diverse. Houses with concrete roofs, unlike houses with asbestos roofing sheets and other materials, were all equipped with ceiling fans and had white-painted ceilings. Moreover, most houses with concrete roofs also had ventilators near the rooftop to help escape warm air.

3.1.2 Time-varying characteristics of the study population

Time spent in cooking-related activities was higher for women than men (e.g., mean self-reported time cooking with an indoor stove were 0.9 (SD 0.7) hours for women vs. 0.1 (SD 0.3) hours for men) (**Figure 2**). There were gender differences in predictors related to occupation (**Figure 2**): on average, while men spent more time in industry (1.7 (SD 3.4) hours) than women (0 (SD 0) hours), the opposite was observed for agricultural labour (1.5 (SD 2.7) hours for women vs. 0.6 (SD 1.9) hours for men) according to wearable camera annotations. Women spent more time at home than men (average time 13.1 (SD 3.7) hours for women vs. 9 (SD 4.3) hours for men) according to GPS, whereas time spent travelling was longer in men (1.4 (SD 1.7) hours for men vs. 0.1 (SD 0.4) hours for women) according to the self-reported diary (**Figure 2**).

Spearman correlations between predictors concerning similar activities and locations measured by different data sources were all positive (**Figure S7**). For instance, correlation between being outdoors in the field (diary) and working in the field (wearable camera) was 0.56. Likewise, the daytime correlation between GVI and GPS-intersected NDVI was positive, yet modest ($\rho_{spearman}$ = 0.26, **Figure S8**).

3.1.3 Characteristics of personal exposures and fixed-site air temperature

Mean personal air temperatures were similar to ambient fixed-site temperatures for daytime hours (31.2 (SD 2.6) ºC personal vs. 30.3 (SD 3.5) ºC ambient) and higher for nighttime hours (28.8 (SD 2.8) ºC personal vs. 23.3 (SD 3.7) ºC ambient) (**Table 2**). No differences in personal exposure to temperature across genders were observed (e.g., daytime mean 31.2 (SD 2.7) ºC in men vs. 31.3 (SD 2.4) ºC in women) (**Table 2**). Most of the variability in personal air temperature occurred within participant: the ICC for daytime personal air temperature was 15% for men and 9% for women; the ICC for nighttime personal air temperature was 9%.

Seasonal and daytime/nighttime contrasts were stronger in ambient fixed-site temperature than in personal (**Figure 3)**. The highest nighttime/daytime and personal/fixed-site temperatures were in the summer season (e.g., mean personal daytime air temperature was 33.9ºC (SD 1.9) in summer) (**Table S2)**. Mean personal temperatures were always higher than ambient fixed-site except during daytime in the summer season, when ambient fixed-site temperatures were warmer than personal (**Table S2**).

3.2 Agreement and association between average ambient fixed-site and personal temperature exposure

Addressing our first objective, there was a substantial discrepancy between average ambient fixed-site and personal temperatures at night (**Figure 4**), when ambient fixed-site temperatures underestimated personal air temperatures (Mean Bias Error, MBE = -5.6ºC). Mean absolute difference during daytime was smaller (MBE = -1.0ºC for men and -0.9ºC for women), although the estimated limits of agreement were wide and larger than ± 5ºC in all cases. Bland-Altman plots suggested presence of proportional bias, e.g., underestimation of personal nighttime air temperatures was smaller for warm summer than for moderately cold winter temperatures.

The strength of the association between average ambient fixed-site and personal temperature was moderate (**Figure 5**). While more than half of the personal temperature exposure variability was explained by ambient fixed-site temperatures in women (R^2_{mar} = 0.51), the proportion for men was lower (R^2_{mar} = 0.30). Estimated slopes were similar for daytime and nighttime temperatures. No effect modification by season was found (interaction between ambient fixed-site temperature and season on personal air temperatures resulted in p-values > 0.2).

3.3 Predictors of personal exposure to air temperature

Addressing our second objective, predictors of nighttime average personal air temperature (**Table 3**) included ambient fixed-site temperature and the geocoded altitude of the household (-1.17 (95% Confidence Interval, CI -1.87, -0.46) ºC for a 100m increase). Other relevant household variables were the ceiling height of the bedroom (-1.61 (95% CI -3.08, -0.15) ºC for 1-meter increase), and a household income greater than 15,000 Indian rupees (0.73 (0, 1.47) ºC). The mean R^2_{mar} of the model in the imputed datasets was 0.48 (range 0.45 to 0.49).

Daytime personal air temperature predictors (**Table 3**) included ambient fixed-site temperature and asbestos roofing sheets for both genders. For women, 1 hour working in the field as measured with the wearable cameras was estimated to increase average daytime personal temperature by 0.1 (95% CI: -0.02, 0.22) ºC. For men, the average altitude measured with the GPS tracks had a negative effect on average personal air temperature (-1.47 (95% CI: -2.38, -0.56) ºC for a 100 meter increase). Moreover, we estimated a 0.21 (95% CI: 0.02, 0.39) ºC personal temperature increase in men for each hour spent in trips according to the GPS. Mean R^2_{mar} for women's models was 0.56 (range 0.53 to 0.58) and for men's it was 0.45 (range 0.41 to 0.48).

Similarly, gender-stratified models for hourly average daytime personal temperature identified ambient fixed-site temperature, bedroom roof material, and altitude as predictors in both men and women's models (**Table S3**). Time spent working according to the self-reported diary (e.g., 0.53ºC (95% CI 0.18, 0.88) per hour worked in women) and time spent outdoors according to the wearable camera (e.g., 0.82ºC (0.47, 1.17) per hour spent outdoors in women) were also predictive for both genders. Working in the field according to the wearable cameras had an effect on average hourly daytime personal temperature only for women; time spent travelling was predictive only for men.

4. Discussion

We investigated the agreement and the association between ambient fixed-site and personal air temperature in a representative sample of the adult population in peri-urban India and identified self-reported and objectively-measured predictors of personal air temperature exposure. Agreement between average personal and fixed-site temperatures was limited, especially at nighttime when personal temperatures were underestimated by ambient fixed-site temperatures. The proportion of average personal nighttime temperature variability explained by ambient fixed-site temperatures was moderate; daytime associations were stronger for women than for men. In addition to ambient fixed-site temperature, we identified several household characteristics predictive of average nighttime personal temperature (e.g., residential altitude), and housing characteristics (e.g., roof material), individual activities (e.g., time spent travelling), and locations (e.g., time spent working in fields) predictive of average daytime personal temperatures. We did not identify UHI, biomass cooking, or greenspace effects.

4.1 Agreement and association with ambient fixed-site temperature exposure

We found that agreement between daytime average personal and ambient fixed-site temperatures was limited and depended on the season. Aligned with our results, previous studies in the US in the general population show that average ambient fixed-site temperature tended to overestimate personal air temperatures in the summer season (Bernhard et al., 2015; Kuras et al., 2015). However, evidence in outdoor workers in the US in the summer season shows slightly warmer mean personal than ambient fixed-site temperatures (Uejio et al., 2018), which were associated with longer time working outdoors. We found that average personal nighttime temperatures were warmer than ambient fixed-site, which agrees with results of a study evaluating indoor and outdoor nighttime summer temperatures in New York (Quinn et al., 2017), even when considering that most of the included households had indoor AC systems. The wide estimated limits of agreements both at daytime and nighttime indicated limited agreement between ambient fixed-site and personal exposures and possibly reflected the influence of other factors affecting personal air temperature.

We identified a higher proportion of average daytime personal temperature variability explained by ambient fixed-site temperatures in women than in men. Although we hypothesised that these differences could be due to higher mobility and a wider range of activities in men, the R^2_{mar} in women's multiple regression models were still higher than men's. Our estimated associations were broadly similar to

previous evidence in the US: Bernhard and colleagues estimated a linear association between average hourly ambient fixed-site and personal temperature of 0.37 (95% CI: 0.35, 0.39) in multiple regression models (Bernhard et al., 2015) (our estimates were 0.32 (95% CI: 0.28, 0.36) for women and 0.38 (95% CI: 0.34, 0.43) for men in multiple hourly daytime regression models).

4.2 Spatial temperature exposure misalignment

Our results provide insights into potential exposure measurement error in epidemiologic studies based on fixed-site exposure assessment. Despite the limited variability in altitude in our study area, we found decreased personal air temperatures for participants dwelling and travelling in more elevated areas. Although the negative association between altitude and temperature is well established for ambient fixed-site temperature (Parsons, 2014), to our knowledge there is no previous evidence of altitude effects in personal air temperature in the general population. Empirically, we found that the change in temperature with elevation above sea level is similar for personal air temperature as what one would expect for ambient fixed-site temperatures based on simple physics (i.e., adiabatic lapse rate). Another spatially-related predictor of personal air temperature is travel. In agreement with our results, studies in the US also found that indoor environments (compared to outdoors) resulted in decreased personal air temperature (Bernhard et al., 2015; Sugg et al., 2018). However, comparability between studies in high and LMICs may be limited due to differences in transport modes and access to in-vehicle AC.

4.3 Household and individual predictors of personal exposure to temperature

Household characteristics were predictive of mean personal air temperature during nighttime and daytime. Housing materials, and especially roof materials, have been identified as an important factor explaining indoor thermal comfort (Latha et al., 2015). Research on the thermal properties of asbestos roofing sheets has demonstrated their good insulating properties (Onyeaju et al., 2012); however, our results indicate that participants dwelling in houses with these roofs experienced higher daytime average temperatures compared to concrete or other materials. We believe that this is because unlike houses with asbestos rooftops, dwellings with concrete roofs were equipped with fans, ventilators, and had white-painted ceilings; and thus, roof type information acted as a marker of housing quality and adaptation to heat. In addition to housing materials, other features of buildings such as building orientation, ventilation and building space usage have also been shown to be important for keeping indoor environments cool (Latha et al., 2015). We found that higher household income was associated with higher mean

temperature in nighttime models. These results were unexpected as previous evidence estimated lower personal air temperature exposure in participants with higher household income (Bernhard et al., 2015), and lower household income has been found to increase vulnerability to heat effects (Son et al., 2019).

We found a positive association between time spent working in agriculture and personal air temperature in daytime models for women, and with time working in any occupation and time spent outdoors in hourly daytime models for men and women. Previous occupational studies have identified outdoor workers in sectors such as agriculture and construction to be at risk of heat effects, especially in LMICs within tropical regions (Xiang et al., 2014) and specifically in India (Venugopal et al., 2016). Even though biomass indoor cooking has been recently reported to affect indoor thermal comfort in Indian rural households (Ravindra et al., 2019), we did not find any effect of cooking on personal air temperature. We hypothesise that this may be because solid fuel use for cooking was mostly conducted outdoors (75% of time) according to wearable camera annotations.

4.4 Effect of greenspace and urban heat island on personal temperature exposure

Even though urban greenspace has been found to have a cooling effect on ambient air temperature (Bowler et al., 2010) and may be an effect modifier in heat epidemiological analyses (Son et al., 2019), we did not find an association between greenspace, either measured by GPS or wearable camera, and personal air temperature. Similar results have been observed in an occupational study in the US (Sugg et al., 2018), where no correlation between land use (including developed areas, open areas, and forests) and personal air temperatures was observed. Cooling effects of greenspace have been found to be fairly localized (Bowler et al., 2010), and so they were likely undetectable for locations in which participants spent short duration of time (e.g., in transit). However, we also did not observe an association with greenspace and nighttime personal air temperature when participants were at home. A possible explanation for this is that findings based on urban areas have limited generalizabiliy to peri-urban and rural areas where greenspace is primarily cropland (Taylor and Hochuli, 2017). Further research is needed to identify the impact of different types of greenspace on personal air temperature outside of urban areas, e.g., differentiating the impact of tree canopies vs. crops.

Although UHI effects have been identified in many cities in south Asia (Kotharkar et al., 2018), we did not find any indication of UHI as explained by time spent within Hyderabad's ring road. This might be because very few participants entered the city and mostly stayed in the peri-urban area. Furthermore,

recent evidence suggests that urban daytime surface temperature in some Indian cities may actually be lower than its surrounding non-urban areas in dry pre-monsoon seasons, when vegetation is scarce and evapotranspiration is low (Shastri et al., 2017). This so-called "urban oasis effect" has also been observed in other geographical regions and has been attributed to low vegetation cover and surface moisture in the surrounding environment (Fan, et al., 2017; Georgescu, et al., 2011).

4.5 Prevention strategies and potential interventions

According to our findings, targets for interventions for health protection should include housing quality and building adaptation to heat to keep indoor environments a cool as possible. In the context of climate change, population growth and rising energy demand in India and other LMICs, improved building adaptation to heat can provide a more sustainable and affordable solution for thermal comfort than the expansion of energy and carbon intensive cooling devices such as ACs (Akpinar-Ferrand and Singh, 2010). The vulnerability of agricultural workers in peri-urban areas supports the need for prevention strategies at the national, regional, and local levels to protect the health of outdoor workers (Nilsson and Kjellstrom, 2010). Finally, heat early warning systems encompassing both rural and urban areas, as well as daytime and nighttime temperatures, should be prioritised and continuously adapted to the changing climate (Hess and Ebi, 2016).

4.6 Strengths and limitations

To our knowledge, this is the first study evaluating personal air temperature in a sample of the general population within a LMIC. This is also the first study including a large range of objectively-measured predictors of personal air temperature, including individual and household characteristics, mobility, activities, and greenspace. The main limitation of the study was the low accuracy of the personal temperature sensor. The manufacturer-reported accuracy of the sensor (± 3ºC) was poorer than temperature sensors available for personal monitoring such as HOBO and iButton (from ± 0.2ºC to ± 1ºC) (Kuras et al., 2017) and showed a slow response time under changes in air temperature in our laboratory experiment. However, all sensors were calibrated before deployment and showed an excellent agreement between each other. Due to the slow response time, we focused our results on average temperature and averaging times of an hour or more. Our estimated regression coefficients were smaller than the manufacturer-reported accuracy: although random error in the measurements (dependent variable in our regression models) could have inflated standard errors of regression coefficients, it is difficult to predict

the effect of the sensor lag on results even after averaging. We had data on AC ownership, but not whether participants used AC during the monitoring. However, only three participants reported having AC, so we expect AC usage to have a limited effect on our results. Finally, we did not have data on other parameters relevant to personal heat exposure (personal radiation, humidity, and air velocity) (Kuras et al., 2017);.

4.7 Conclusions

R^2_{mar} between ambient fixed-site and personal air temperature indicate that ambient fixed-site temperature is only a moderately useful proxy of personal temperature in epidemiologic studies in the context of a peri-urban area in India. Our results highlight additional factors that should be taken into account in epidemiological studies, for example altitude – either through spatially-resolved ambient fixed-site temperature that accounts for altitude, or by exploring exposure measurement error by altitude in studies based on fixed site monitoring. In addition to demographics, our results provide further evidence that several additional factors representing differential exposure measurement error should be explored in epidemiological studies based on fixed site monitors including: 1) housing materials and dimensions 2) occupation 3) socio-economic factors 4) mobility and 5) time spent indoors/outdoors.

5. Acknowledgements

We thank all CHAI participants as well as the field team who collected the information used in this study. We acknowledge the EU Copernicus Programme (Sentinel 2 mission) for the remote sensing data and the openstreetmap community for the study area geometries we used. We would also like to thank Mar Viana from IDAEA-CSIC for providing microPEM filters, Lidia Cañas and Sílvia Borràs for the laboratory equipment needed for temperature experiments, and the Research Quality Service from University of Barcelona (UB) from which we rented the Testo thermohygrometer.

6. Funding

This research was funded by the European Research Council under ERC Grant Agreement number 336167 for the CHAI Project. Cathryn Tonne was funded through a Ramón y Cajal fellowship (RYC-2015-17402) awarded by the Spanish Ministry of Economy and Competitiveness. None of the funding sources had a role in study design; in the collection, analysis and interpretation of data; in the writing of the report; and in the decision to submit the article for publication.

7. References

Akpinar-Ferrand, E., Singh, A., 2010. Modeling increased demand of energy for air conditioners and consequent CO2 emissions to minimize health risks due to climate change in India. Environ. Sci. Policy 13, 702–712. https://doi.org/https://doi.org/10.1016/j.envsci.2010.09.009

Basu, R., Samet, J.M., 2002. An exposure assessment study of ambient heat exposure in an elderly population in Baltimore, Maryland. Environ. Health Perspect. 110, 1219–1224. https://doi.org/10.1289/ehp.021101219

Bates, D., Mächler, M., Bolker, B., Walker, S., 2015. Fitting Linear Mixed-Effects Models Using {lme4}. J. Stat. Softw. 67, 1–48. https://doi.org/10.18637/jss.v067.i01

Beck, H.E., Zimmermann, N.E., McVicar, T.R., Vergopolan, N., Berg, A., Wood, E.F., 2018. Present and future Köppen-Geiger climate classification maps at 1-km resolution. Sci. Data 5, 180214.

Bernhard, M.C., Kent, S.T., Sloan, M.E., Evans, M.B., McClure, L.A., Gohlke, J.M., 2015. Measuring personal heat exposure in an urban and rural environment. Environ. Res. 137, 410–418. https://doi.org/https://doi.org/10.1016/j.envres.2014.11.002

Bland, J.M., Altman, D.G., 2007. Agreement Between Methods of Measurement with Multiple Observations Per Individual. J. Biopharm. Stat. 17, 571–582. https://doi.org/10.1080/10543400701329422

Bowler, D.E., Buyung-Ali, L., Knight, T.M., Pullin, A.S., 2010. Urban greening to cool towns and cities: A systematic review of the empirical evidence. Landsc. Urban Plan. 97, 147–155. https://doi.org/https://doi.org/10.1016/j.landurbplan.2010.05.006

Brook, R.D., Shin, H.H., Bard, R.L., Burnett, R.T., Vette, A., Croghan, C., Williams, R., 2011. Can personal exposures to higher nighttime and early-morning temperatures increase blood pressure? J. Clin. Hypertens. (Greenwich). 13, 881–888. https://doi.org/10.1111/j.1751-7176.2011.00545.x

Donaire-gonzalez, D., Valentín, A., Nazelle, A. De, Ambros, A., 2016. Benefits of Mobile Phone Technology for Personal Environmental Monitoring. JMIR Mhealth Uhealth 4. https://doi.org/10.2196/mhealth.5771

ESA, n.d. Copernicus Open Access Hub [WWW Document]. URL https://scihub.copernicus.eu/ (accessed 1.10.19).

Fan, C., Myint, S.W., Kaplan, S., Middel, A., Zheng, B., Rahman, A.,Huang, H.-P, , Brazel, A., Blumberg, D.G. Understanding the impact of urbanization on surface urban heat islands—a longitudinal analysis of the oasis effect in subtropical desert cities. Remote Sensing, 9(7), 672. https://doi.org/10.3390/rs9070672

Fu, S.H., Gasparrini, A., Rodriguez, P.S., Jha, P., 2018. Mortality attributable to hot and cold ambient temperatures in India: a nationally representative case-crossover study. PLOS Med. 15, 1–17. https://doi.org/10.1371/journal.pmed.1002619

Gasparrini, A., Guo, Y., Hashizume, M., Lavigne, E., Zanobetti, A., Schwartz, J., Tobias, A., Tong, S., Rocklöv, J., Forsberg, B., Leone, M., De Sario, M., Bell, M.L., Guo, Y.-L.L., Wu, C., Kan, H., Yi, S.-M., de Sousa Zanotti Stagliorio Coelho, M., Saldiva, P.H.N., Honda, Y., Kim, H., Armstrong, B., 2015. Mortality risk attributable to high and low ambient temperature: a multicountry observational study. Lancet 386, 369–375. https://doi.org/10.1016/S0140-6736(14)62114-0

Georgescu, M., Moustaoui, M., Mahalov, A., & Dudhia, J. (2011). An alternative explanation of the semiarid urban area "oasis effect". Journal of Geophysical Research: Atmospheres, 116(D24).

Green, H., Bailey, J., Schwarz, L., Vanos, J., Ebi, K., Benmarhnia, T., 2019. Impact of heat on mortality and morbidity in low and middle income countries: A review of the epidemiological evidence and considerations for future research. Environ. Res. 171, 80–91. https://doi.org/https://doi.org/10.1016/j.envres.2019.01.010

Grolemund, G., Wickham, H., 2011. Dates and Times Made Easy with {lubridate}. J. Stat. Softw. 40, 1–25.

Hess, J.J., Ebi, K.L., 2016. Iterative management of heat early warning systems in a changing climate. Ann. N. Y. Acad. Sci. 1382, 21–30. https://doi.org/10.1111/nyas.13258

Hijmans, R.J., 2019. raster: Geographic Data Analysis and Modeling.

Hunziker, P., 2017. velox: Fast Raster Manipulation and Extraction.

Iannone, R., 2019. DiagrammeR: Graph/Network Visualization.

Ingole, V., Kovats, S., Schumann, B., Hajat, S., Rocklöv, J., Juvekar, S., Armstrong, B., 2017. Socioenvironmental factors associated with heat and cold-related mortality in Vadu HDSS, western India: a population-based case-crossover study. Int. J. Biometeorol. 61, 1797–1804. https://doi.org/10.1007/s00484-017-1363-8

IPCC, 2014. The IPCC's Fifth Assessment Report: What's in it for South Asia. Geneva, Switzerland.

Jaeger, B., 2017. r2glmm: Computes R Squared for Mixed (Multilevel) Models.

Kinra, S., Radha Krishna, K. V, Kuper, H., Rameshwar Sarma, K. V, Prabhakaran, P., Gupta, V., Walia, G.K., Bhogadi, S., Kulkarni, B., Kumar, A., Aggarwal, A., Gupta, R., Prabhakaran, D., Reddy, K.S., Davey Smith, G., Ben-Shlomo, Y., Ebrahim, S., 2014. Cohort Profile: Andhra Pradesh Children and Parents Study (APCAPS). Int. J. Epidemiol. 43, 1417–1424. https://doi.org/10.1093/ije/dyt128

Kotharkar, R., Ramesh, A., Bagade, A., 2018. Urban Heat Island studies in South Asia: A critical review. Urban Clim. 24, 1011–1026. https://doi.org/https://doi.org/10.1016/j.uclim.2017.12.006

Kuras, E.R., Hondula, D.M., Brown-Saracino, J., 2015. Heterogeneity in individually experienced temperatures (IETs) within an urban neighborhood: insights from a new approach to measuring heat exposure. Int. J. Biometeorol. 59, 1363–1372. https://doi.org/10.1007/s00484-014-0946-x

Kuras, E.R., Richardson, M.B., Calkins, M.M., Ebi, K.L., Hess, J.J., Kintziger, K.W., Jagger, M.A., Middel, A., Scott, A.A., Spector, J.T., Uejio, C.K., Vanos, J.K., Zaitchik, B.F., Gohlke, J.M., Hondula, D.M., 2017. Opportunities and Challenges for Personal Heat Exposure Research. Environ. Health Perspect. 125, 85001. https://doi.org/10.1289/EHP556

Latha, P.K., Darshana, Y., Venugopal, V., 2015. Role of building material in thermal comfort in tropical climates – A review. J. Build. Eng. 3, 104–113. https://doi.org/https://doi.org/10.1016/j.jobe.2015.06.003

Li, X., Zhang, C., Li, W., Kuzovkina, Y.A., Weiner, D., 2015. Who lives in greener neighborhoods? The distribution of street greenery and its association with residents' socioeconomic conditions in Hartford, Connecticut, USA. Urban For. Urban Green. 14, 751–759.

https://doi.org/https://doi.org/10.1016/j.ufug.2015.07.006

Liberto, T. Di, 2015. India heat wave kills thousands [WWW Document]. URL https://www.climate.gov/news-features/event-tracker/india-heat-wave-kills-thousands (accessed 5.22.19).

Lioy, P.J., 2010. Exposure Science: A View of the Past and Milestones for the Future. Environ. Health Perspect. 118, 1081–1090. https://doi.org/10.1289/ehp.0901634

Louis, J., Debaecker, V., Pflug, B., Main-Knorn, M., Bieniarz, J., Mueller-Wilm, U., Cadau, E., Gascon, F., 2016. Sentinel-2 SEN2COR: L2A processor for users, in: Proceedings of the Living Planet Symposium, Prague, Czech Republic. pp. 9–13.

Mastrucci, A., Byers, E., Pachauri, S., Rao, N.D., 2019. Improving the SDG energy poverty targets: Residential cooling needs in the Global South. Energy Build. 186, 405–415. https://doi.org/https://doi.org/10.1016/j.enbuild.2019.01.015

Milà, C., Salmon, M., Sanchez, M., Ambrós, A., Bhogadi, S., Sreekanth, V., Nieuwenhuijsen, M., Kinra, S., Marshall, J.D., Tonne, C., 2018. When, Where, and What? Characterizing Personal PM2.5 Exposure in Periurban India by Integrating GPS, Wearable Camera, and Ambient and Personal Monitoring Data. Environ. Sci. Technol. 52, 13481–13490. https://doi.org/10.1021/acs.est.8b03075

MIT Senseable City Lab, n.d. Treepedia package for public use [WWW Document]. URL https://github.com/mittrees/Treepedia_Public (accessed 8.1.19).

Murari, K.K., Ghosh, S., Patwardhan, A., Daly, E., Salvi, K., 2015. Intensification of future severe heat waves in India and their effect on heat stress and mortality. Reg. Environ. Chang. 15, 569–579. https://doi.org/10.1007/s10113-014-0660-6

Nakagawa, S., Schielzeth, H., 2013. A general and simple method for obtaining R2 from generalized linear mixed-effects models. Methods Ecol. Evol. 4, 133–142.

Nilsson, M., Kjellstrom, T., 2010. Climate change impacts on working people: how to develop prevention policies. Glob. Health Action 3, 10.3402/gha.v3i0.5774. https://doi.org/10.3402/gha.v3i0.5774

Onyeaju, M.C., Osarolube, E., Chukwuocha, E.O., Ekuma, C.E., Omasheye, G.A.J., 2012. Comparison of

the thermal properties of asbestos and polyvinylchloride (PVC) ceiling sheets. Mater. Sci. Appl 3, 240–244.

Parsons, K., 2014. Human thermal environments: the effects of hot, moderate, and cold environments on human health, comfort, and performance. CRC press.

Pebesma, E., 2018. sf: Simple Features for R.

Pinheiro, J., Bates, D., DebRoy, S., Sarkar, D., R Core Team, 2018. {nlme}: Linear and Nonlinear Mixed Effects Models.

Quinn, A., Kinney, P., Shaman, J., 2017. Predictors of summertime heat index levels in New York City apartments. Indoor Air 27, 840–851. https://doi.org/10.1111/ina.12367

R Core Team, 2019. R: A Language and Environment for Statistical Computing.

Ravindra, K., Agarwal, N., Kaur-Sidhu, M., Mor, S., 2019. Appraisal of thermal comfort in rural household kitchens of Punjab, India and adaptation strategies for better health. Environ. Int. 124, 431–440. https://doi.org/https://doi.org/10.1016/j.envint.2018.12.059

Runkle, J.D., Cui, C., Fuhrmann, C., Stevens, S., Del Pinal, J., Sugg, M.M., 2019. Evaluation of wearable sensors for physiologic monitoring of individually experienced temperatures in outdoor workers in southeastern U.S. Environ. Int. 129, 229–238. https://doi.org/https://doi.org/10.1016/j.envint.2019.05.026

Salve, H .R., Parthasarathy , R., Krishnan, A., Pattanaik, D.R., 2018. Impact of ambient air temperature on human health in India. Rev. Environ. Health. https://doi.org/10.1515/reveh-2018-0024

Salmon, M., 2017. rtimicropem: CHAI data cleaning [WWW Document]. URL https://ropensci.github.io/rtimicropem/articles/chai_data_cleaning.html

Salmon, M., 2016. riem: Accesses Weather Data from the Iowa Environment Mesonet.

Salmon, M., 2013. watchme: R package that supports the analysis of images annotations [WWW Document].

Salmon, M., Milà, C., Bhogadi, S., Addanki, S., Madhira, P., Muddepaka, N., Mora, A., Sanchez, M.,

Kinra, S., Sreekanth, V., Doherty, A., Marshall, J.D., Tonne, C., 2018. Wearable camera-derived microenvironments in relation to personal exposure to PM2.5. Environ. Int. 117, 300–307.

Sanchez, M., Ambros, A., Salmon, M., Bhogadi, S., Wilson, R.T., Kinra, S., Marshall, J.D., Tonne, C., 2017. Predictors of daily mobility of adults in peri-urban South India. Int. J. Environ. Res. Public Health 14, 783.

Shastri, H., Barik, B., Ghosh, S., Venkataraman, C., Sadavarte, P., 2017. Flip flop of Day-night and Summer-Winter Surface Urban Heat Island Intensity in India. Sci. Rep. 7, 40178.

Son, J., Liu, J.C., Bell, M.L., 2019. Temperature-related mortality: A systematic review and investigation of effect modifiers. Environ. Res. Lett.

Steinle, S., Reis, S., Sabel, C.E., 2013. Quantifying human exposure to air pollution—Moving from static monitoring to spatio-temporally resolved personal exposure assessment. Sci. Total Environ. 443, 184–193.

Sugg, M.M., Fuhrmann, C.M., Runkle, J.D., 2018. Temporal and spatial variation in personal ambient temperatures for outdoor working populations in the southeastern USA. Int. J. Biometeorol. 62, 1521–1534. https://doi.org/10.1007/s00484-018-1553-z

Sugg, M.M., Stevens, S., Runkle, J.D., 2019. Estimating personal ambient temperature in moderately cold environments for occupationally exposed populations. Environ. Res. 173, 497–507. https://doi.org/https://doi.org/10.1016/j.envres.2019.03.066

Taylor, L., Hochuli, D.F., 2017. Defining greenspace: Multiple uses across multiple disciplines. Landsc. Urban Plan. 158, 25–38. https://doi.org/https://doi.org/10.1016/j.landurbplan.2016.09.024

Tonne, C., Basagaña, X., Chaix, B., Huynen, M., Hystad, P., Nawrot, T.S., Slama, R., Vermeulen, R., Weuve, J., Nieuwenhuijsen, M., 2017a. New frontiers for environmental epidemiology in a changing world. Environ. Int. 104, 155–162. https://doi.org/10.1016/j.envint.2017.04.003

Tonne, C., Salmon, M., Sanchez, M., Sreekanth, V., Bhogadi, S., Sambandam, S., Balakrishnan, K., Kinra, S., Marshall, J.D., 2017b. Integrated assessment of exposure to PM2.5 in South India and its relation with cardiovascular risk: Design of the CHAI observational cohort study. Int. J. Hyg. Environ. Health 220, 1081–1088.

Uejio, C.K., Morano, L.H., Jung, J., Kintziger, K., Jagger, M., Chalmers, J., Holmes, T., 2018. Occupational heat exposure among municipal workers. Int. Arch. Occup. Environ. Health 91, 705–715. https://doi.org/10.1007/s00420-018-1318-3

van Buuren, S., Groothuis-Oudshoorn, K., 2011. mice: Multivariate Imputation by Chained Equations in R. J. Stat. Softw. 45, 1–67.

Venugopal, V., Chinnadurai, S.J., Lucas, A.R., Kjellstrom, T., 2016. Occupational Heat Stress Profiles in Selected Workplaces in India. Int. J. Environ. Res. Public Heal. . https://doi.org/10.3390/ijerph13010089

Wickham, H., 2017. tidyverse: Easily Install and Load "Tidyverse" Packages.

Wickham, H., 2016. ggplot2: Elegant Graphics for Data Analysis. Springer-Verlag New York.

Wood, S., 2006. Generalized additive models: an introduction with R. CRC press.

Xiang, J., Bi, P., Pisaniello, D., Hansen, A., 2014. Health impacts of workplace heat exposure: an epidemiological review. Ind. Health 52, 91–101. https://doi.org/10.2486/indhealth.2012-0145

Table 1 Study population time-invariant individual and household characteristics.

	All (n=50)	Women (n=25)	Men (n=25)
Age - AM (SD)	43.2 (13.7)	47.2 (9.1)	39.2 (16.4)
Occupation - N (%)			
Manual	42 (84%)	21 (84%)	21 (84%)
Non-manual	2 (4%)	1 (4%)	1 (4%)
Unemployed	6 (12%)	3 (12%)	3 (12%)
Education - N (%)			
Illiterate	29 (58%)	20 (80%)	9 (36%)
Primary studies	8 (16%)	3 (12%)	5 (20%)
Secondary/Superior studies	13 (26%)	2 (8%)	11 (44%)
Household income > 15,000 Indian Rupees - N (%)	12 (24%)	6 (24%)	6 (24%)
Number of household assets - AM (SD)	4.2 (1.5)	4.4 (1.8)	4 (1.3)
Air conditioning at home - N (%)	3 (6%)	2 (8%)	1 (4%)
Household type - N (%)			
Separate house	43 (86%)	23 (92%)	20 (80%)
Shared house/apartment	7 (14%)	2 (8%)	5 (20%)
Bedroom wall material - N (%)			
Brick	43 (86%)	22 (88%)	21 (84%)
Mud/clay	7 (14%)	3 (12%)	4 (16%)
Bedroom floor material - N (%)			
Cement	11 (22%)	6 (24%)	5 (20%)
Mud/stone	22 (44%)	9 (36%)	13 (52%)
Tiles	17 (34%)	10 (40%)	7 (28%)
Bedroom roof material - N (%)			
Tiles/grass	11 (22%)	5 (20%)	6 (24%)
Asbestos sheets	15 (30%)	7 (28%)	8 (32%)
Concrete	24 (48%)	13 (52%)	11 (44%)
Bedroom size (m^2) - AM (SD)	12.8 (4.4)	12.6 (3.8)	13 (4.9)
Bedroom ceiling height (m) - AM (SD)	3 (0.3)	3.1 (0.3)	2.9 (0.3)
Bedroom number of windows - AM (SD)	0.9 (0.9)	1.1 (1)	0.8 (0.8)
Residential altitude above the sea level (m) - AM (SD)	570.2 (47.1)	575.9 (48.6)	564.5 (45.8)

Table 2 Summary statistics of average daytime (6am-10pm) and nighttime (10pm-6am) ambient and personal temperature exposures.

Exposures	**min**	**Q25**	**mean**	**median**	**Q75**	**max**	**sd**
Average personal daytime temperature (ºC)	24.2	29.4	31.2	31.4	32.9	38.5	2.6
Average ambient daytime temperature (ºC)	24.8	27.6	30.3	29.7	32.3	42.6	3.5
Average personal nighttime temperature (ºC)	19.9	26.9	28.8	29.0	30.5	35.7	2.8
Average ambient nighttime temperature (ºC)	14.9	21.0	23.3	23.6	25.4	32.5	3.7

Table 3 Predictors of average nighttime (10pm - 6am) and gender-stratified predictors of average daytime (6am - 10pm) of personal exposure to air temperature.

Temperature predictors	**Data source**	**Change in ºC (95% CI)**
Nighttime (n=207)		
Ambient temperature (1ºC increase)	Ambient fixed site	0.5 (0.42, 0.58)
Residential altitude (100m increase)	GPS	-1.17 (-1.87, -0.46)
Bedroom ceiling height (1m increase)	Baseline questionnaire	-1.61 (-3.08, -0.15)
Household income >15,000 Indian rupees (vs. below)	Baseline questionnaire	0.73 (0, 1.47)
Daytime women (n = 117)		
Ambient temperature (1ºC increase)	Ambient fixed site	0.47 (0.39, 0.55)
Asbestos sheet bedroom roof (vs. tiles/grass)	Baseline questionnaire	1.34 (0.21, 2.47)
Concrete bedroom roof (vs. tiles/grass)	Baseline questionnaire	0.14 (-0.88, 1.16)
Working in field (1h increase)	Wearable camera	0.1 (-0.02, 0.22)
Men (n = 110)		
Ambient temperature (1ºC increase)	Ambient fixed site	0.45 (0.32, 0.58)
Asbestos sheet bedroom roof (vs. tiles/grass)	Baseline questionnaire	0.91 (-0.21, 2.04)
Concrete bedroom roof (vs. tiles/grass)	Baseline questionnaire	-0.67 (-1.73, 0.39)
Shared house/Apartment (vs. separate house)	Baseline questionnaire	1.22 (-0.01, 2.45)
Individual altitude (100m increase)	GPS	-1.47 (-2.38, -0.56)
Travelling (1h increase)	GPS	0.21 (0.02, 0.39)

Linear mixed models (random intercept per participant) fit to multiply imputed datasets and pooled using Rubin's rules.

Figure 1 Data integration graphical summary.

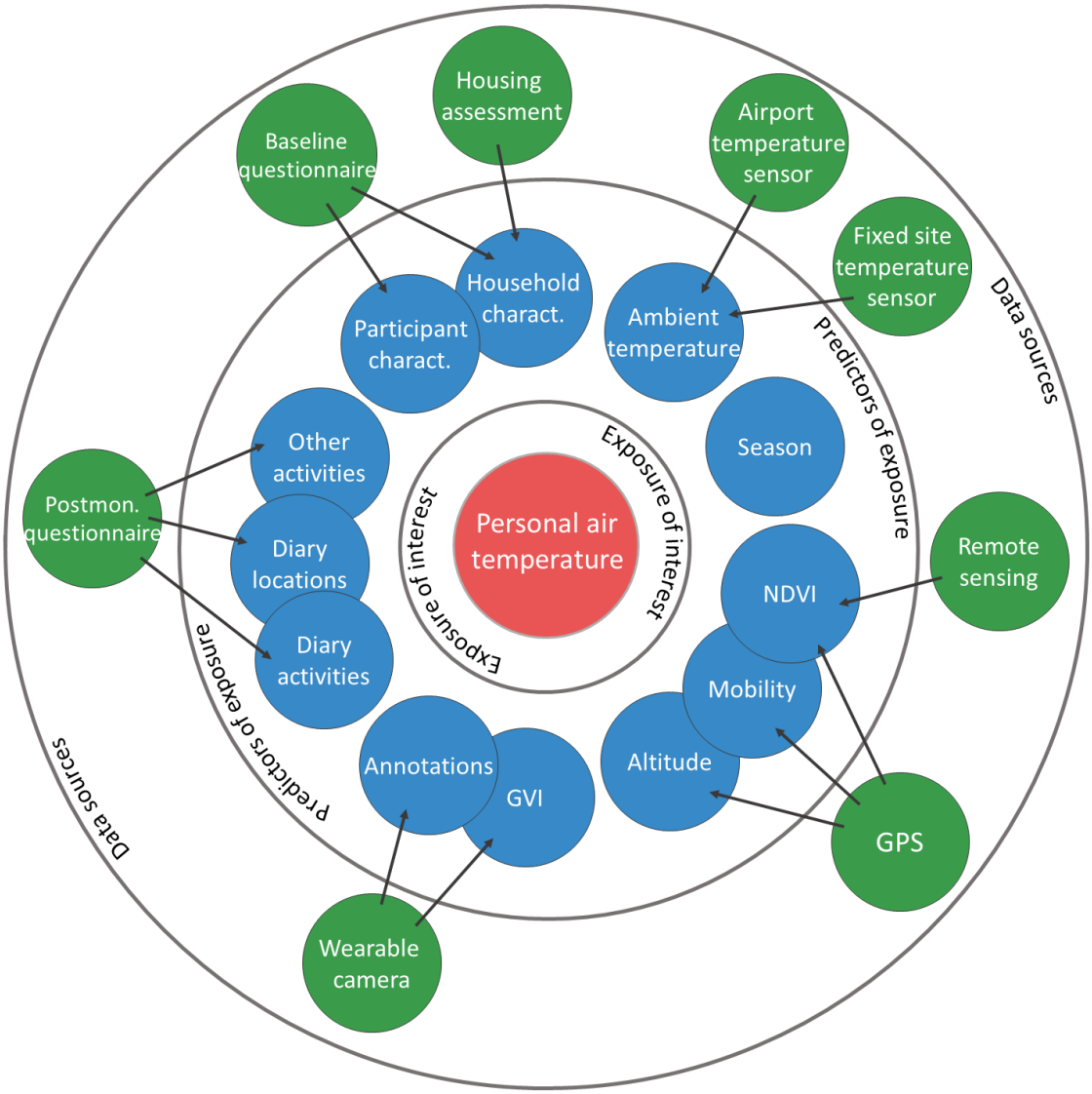

Figure 2 Daytime time-varying activities and locations by data source and gender.

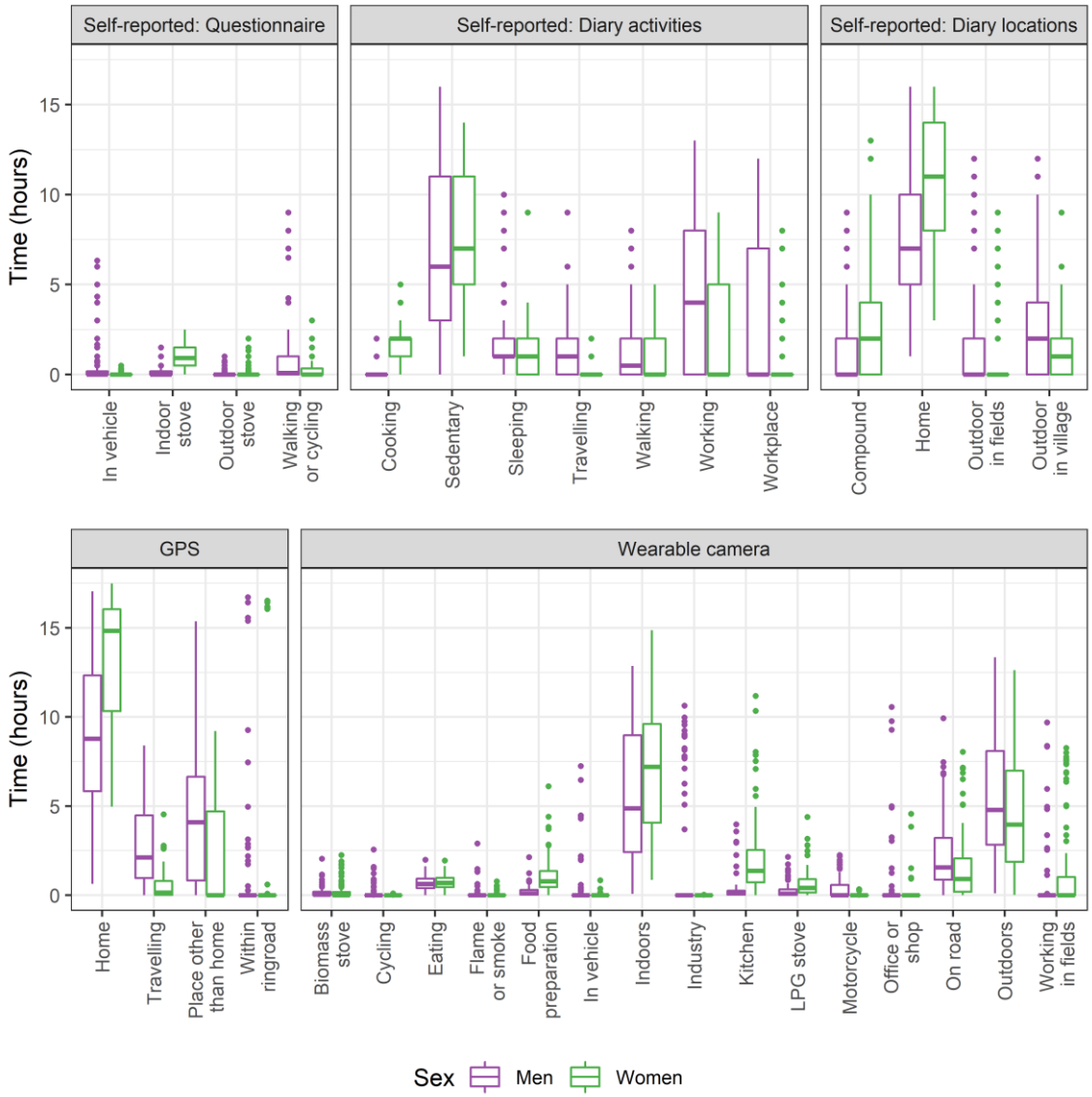

The lower and upper hinges of the box correspond to the 25th and 75th percentiles, the bold bar represents the median. Whiskers defined as the highest/lowest value within 1.5*Interquartile range from the hinge, values beyond that are plotted as points representing outliers.

Figure 3 Temporal patterns of personal and ambient temperature exposure by season.

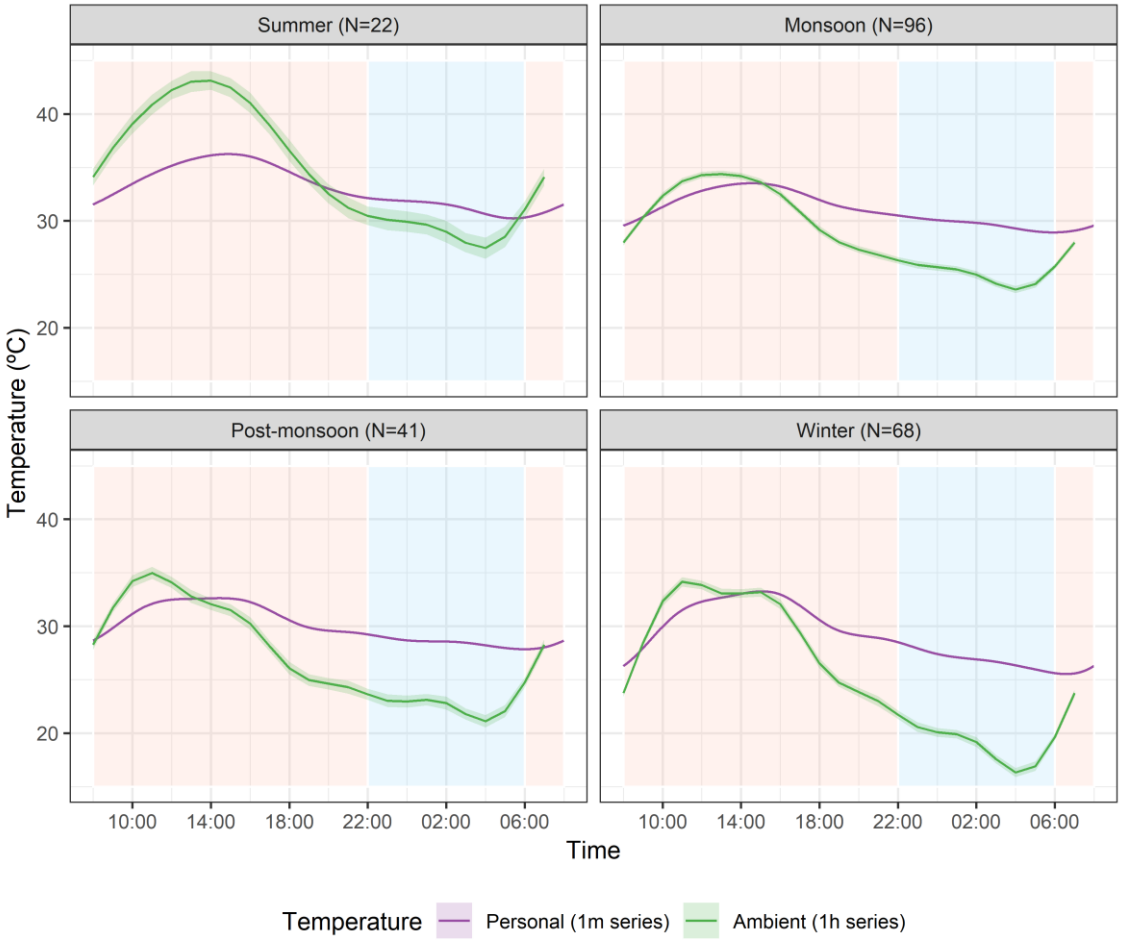

Orange and blue shaded areas represent daytime (6am – 10pm) and nighttime (10pm - 6am) as defined in this study. Estimates and 95% CI (shaded bands) were derived with generalized additive models with a smooth term for the time of day.

Figure 4 Bland-Altman plots of average ambient and personal temperature exposure.

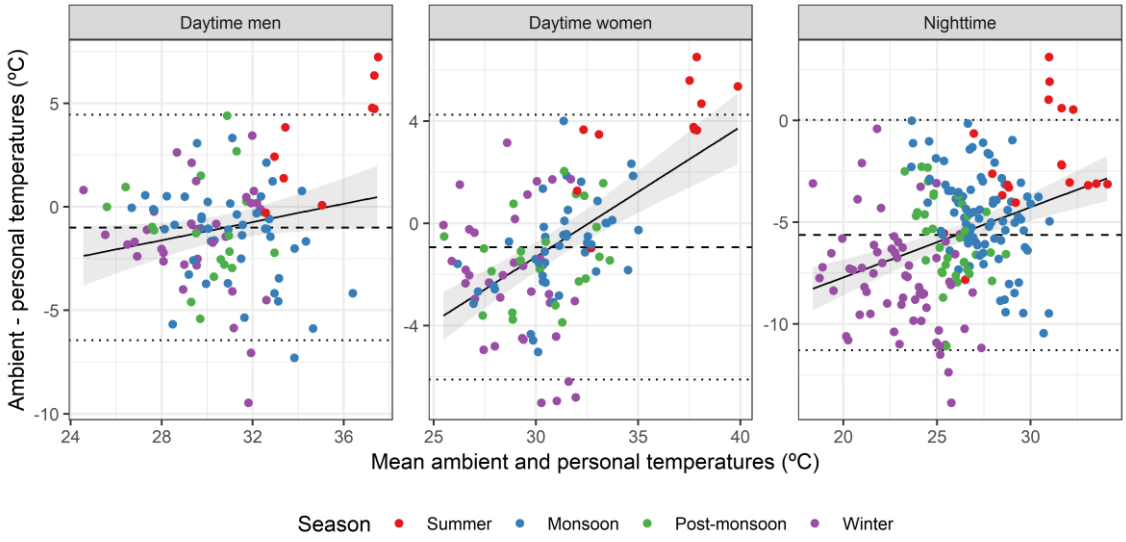

The dashed line represents the mean difference between ambient and personal temperature exposures.

Dotted lines representing limits of agreement calculated following Bland and Altman methods for repeated measures.

The bold line represents the linear fit (mixed model with a random intercept per participant) of the mean personal and ambient temperature on the difference between ambient and personal temperature (shaded area represents its 95% CI).

Figure 5 Associations between average ambient and personal temperature exposure.

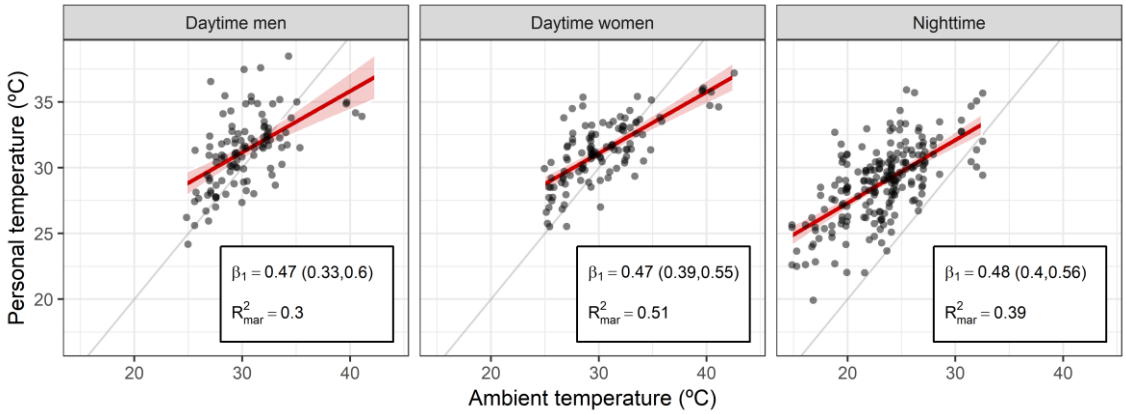

Linear mixed models with a random intercept per participant. R^2_{mar} (or marginal R^2) corresponds to the proportion of personal temperature variance explained by fixed factors, i.e. ambient temperature.

Supplementary material

Predictors of personal exposure to air temperature in peri-urban India

Carles Milà[a], Ariadna Curto[a], Asya Dimitrova[a], V. Sreekanth[bc],
Sanjay Kinra[d], Julian D. Marshall[b], Cathryn Tonne[a*]

a. ISGlobal, Universitat Pompeu Fabra, CIBER Epidemiología y Salud Pública, Barcelona, Spain

b. Department of Civil and Environmental Engineering, University of Washington, Seattle, WA, USA

c. Center for Study of Science, Technology & Policy, Bengaluru 560 094, India

d. Department of Non-communicable Disease Epidemiology, London School of Hygiene and Tropical Medicine, London, UK

* Corresponding autor: Cathryn Tonne

cathryn.tonne@isglobal.org

ISGlobal, Universitat Pompeu Fabra, CIBER Epidemiología y Salud Pública, Doctor Aiguader 88, 08003 Barcelona, Spain

Number of figures: 8

Number of tables: 3

Number of supplementary methods: 3

Figure S1 Map of the study area.

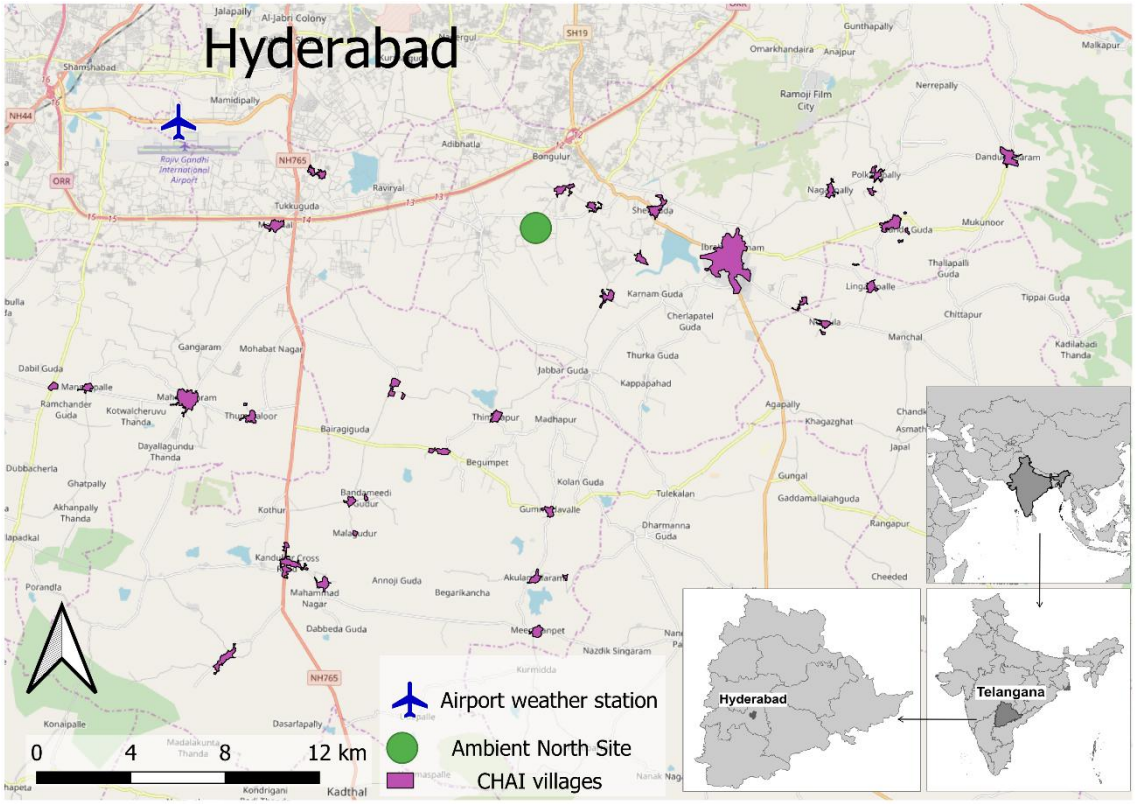

OSM used as background map.

Figure S2 CHAI panel participant carrying the personal monitoring devices.

Personal monitoring devices consisted of a particulate air pollution monitor including an ambient temperature sensor (left) and a wearable camera (centre). A GPS monitor and an accelerometer were placed inside the secured rucksack.

Figure S3 Personal temperature time series (1-minute averages) by season.

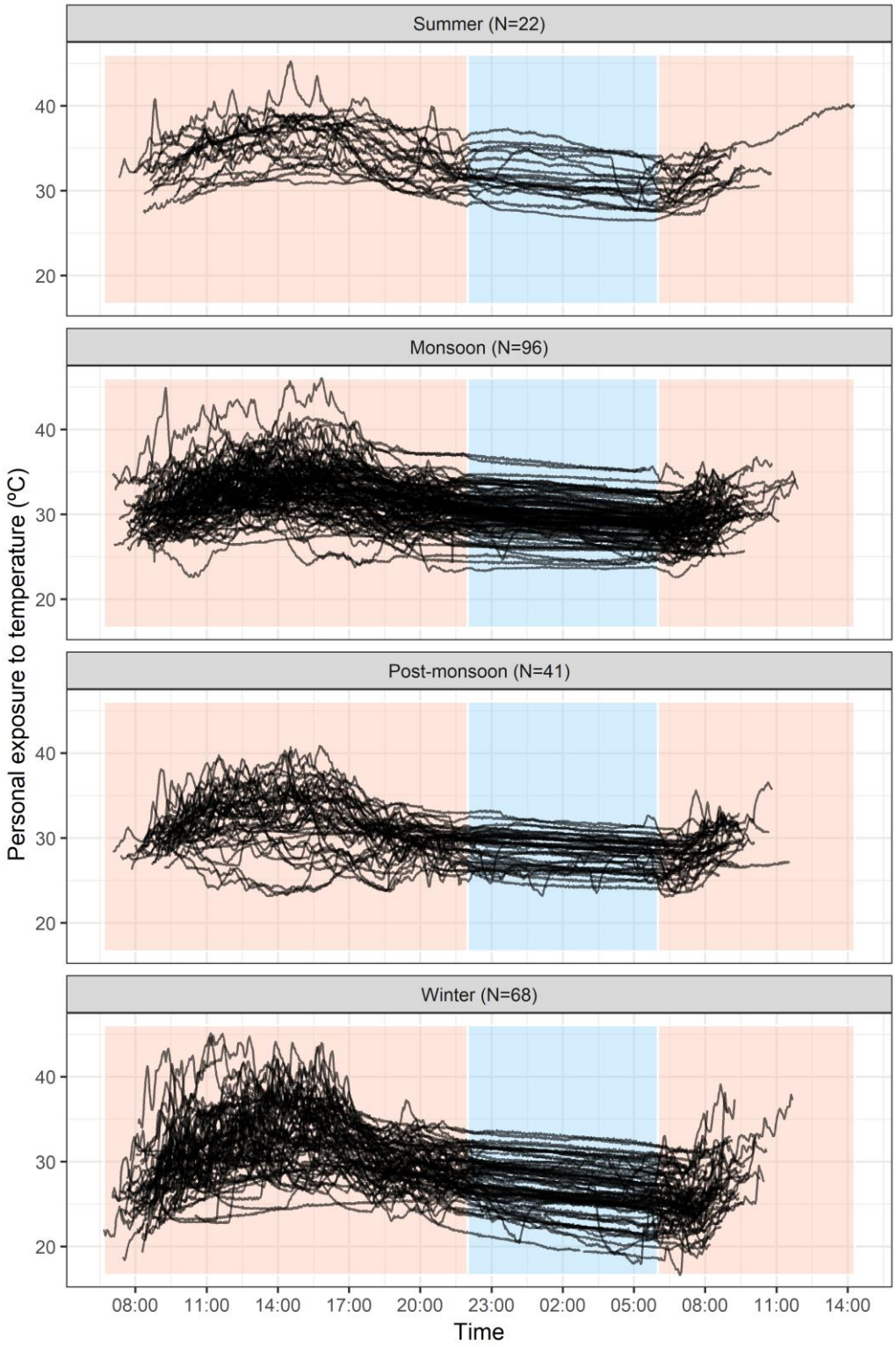

Orange and blue shaded areas represent daytime and nighttime as defined in this study. Participants who did not sleep and who have been removed in main nighttime analyses are also included in this figure.

Methods S1 MicroPEM temperature sensor experiment.

Date: 2019-02-14

Location: Institut Bonanova. Passeig Circumval·lació, 8, Barcelona 08003

Researchers: Ariadna Curto, Carles Milà

Materials

- Four microPEM (v3.2A) devices (all of them had a Teflon 25-mm filter loaded).
- Small screwdriver (to open microPEM and insert batteries).
- Thermohygrometer Testo 635-2 (calibrated on January 2019 by ENAC, an accredited Spanish laboratory). Temperature measurement range and accuracy: -20 to 70ºC ± 0.3 (0.1 resolution).
- Portable printer from Testo.
- Laptop computer with microPEM docking station software (Version 2.0.6236.20371).
- Selecta "Incubat" heater (adjustable temperatures from room temperature +5ºC to 80ºC).
- Batteries (Eneloop AA) and USB cable.

Description

Before the experiment:

- We rented the Testo thermohygrometer from University of Barcelona for three days as a group member (need to check availability and receive training in advance).
- We loaded microPEM with 25-mm Teflon filters and checked they were working well by conducting short samplings.
- We checked availability of the laboratory and heater.

During the experiment:

10:00 We deployed the Testo Thermohygrometer and checked ambient conditions of the laboratory (17.5°C, 48.6% RH).

10:05 We inserted batteries in the MicroPEM devices and assessed their functioning.

10:15 We calibrated the MicroPEM temperature by connecting the devices to the laptop and comparing readings in the MicroPEM docking station software and those of the Testo device.

10:30 We initialised the data recording of the four microPEM devices (double checking that the green light on the top was blinking) and the Testo Thermohygrometer (double checking that the word "Final" appeared in the bottom-right screen). Testo was set to record one reading every 1 minute whereas microPEM recordings were at 30s intervals.

The four microPEM tested and the Testo thermohygrometer used in the experiment.

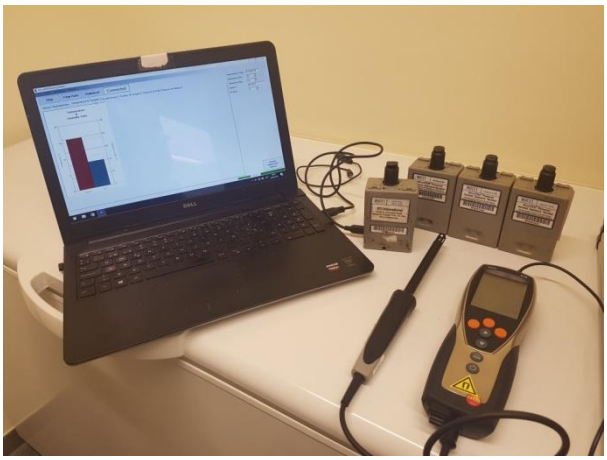

MicroPEM temperature calibration before experiment.

10:35 We placed the devices inside the heater with microPEM inlets (where the temperature sensors are located) as close to each other as possible. Care was taken to make sure the temperature probe was not touching the grill.

Heater used in the experiment. Left picture is with the two doors open (glass door and main door).
Right picture is with the door closed (temperature probe was inside the heater but monitor was kept outside).

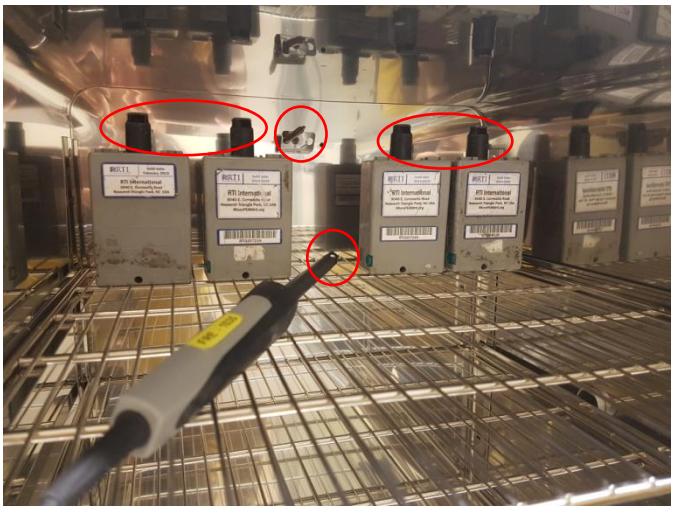

A closer view of the inside of the heater. Red cercles represent where the sensors were located: micoPEM (black caps), temperature probe, and temperature sensor from the heater.

10:45 We turned on the heater and increased temperature to 25ºC.

11:15 We increased heater temperature to 30ºC.

11:45 We increased heater temperature to 35ºC.

12:15 We increased heater temperature to 40ºC.

12:50 We increased heater temperature to 45ºC.

13:15 We increased heater temperature to 50ºC.

13:45 We turned off the heater, extracted the devices, and placed them on a surface exposed to ambient temperature.

14:30 We stopped the devices. Ambient conditions were 19.4°C, 44.2% RH according to Testo.

After the experiment:

- We downloaded microPEM readings and printed the measurements from Testo.
- We computed temperature 1-minute averages to align microPEMs and Testo readings.
- We generated a graph of the resulting time series and calculated statistics to evaluate the objectives of the experiment.

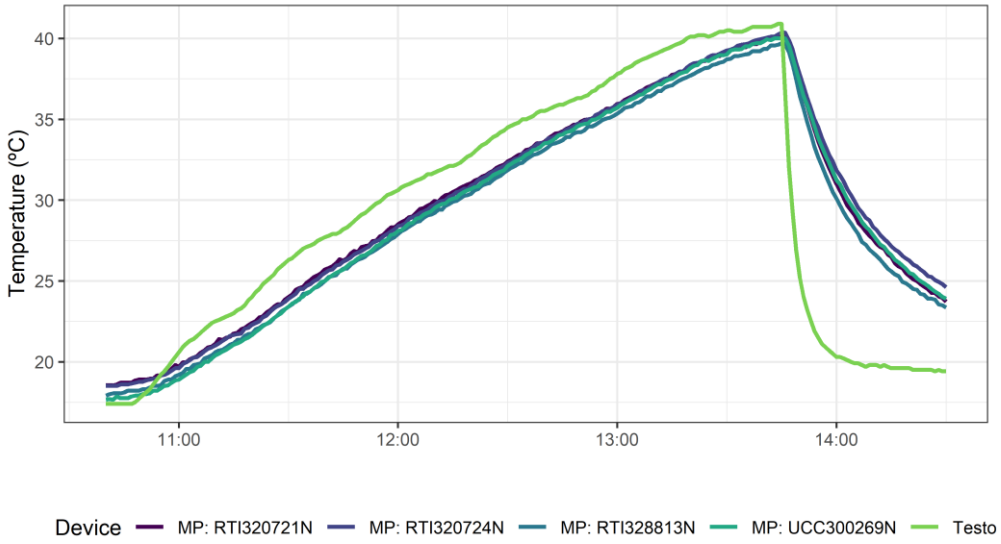

Plot showing the temperature readings from the four co-located units of the MicroPEM (MP) and the reference monitor (Testo) during the experiment.

Results

The four MicroPEM devices showed a very good agreement between each other (ICC = 1). Compared to Testo, they showed a slower responsiveness to the progressive increases in temperature, although the difference was small (RMSE ranged from 1.7 to 2.1 depending on the device). When temperature suddenly dropped due to the extraction of the devices from the heater, the four microPEM showed a poor responsiveness. They took 45 minutes to reduce temperature by 15ºC (actual temperature drop was approximately 20ºC according to Testo).

Figure S4 Altitude of daytime GPS tracks.

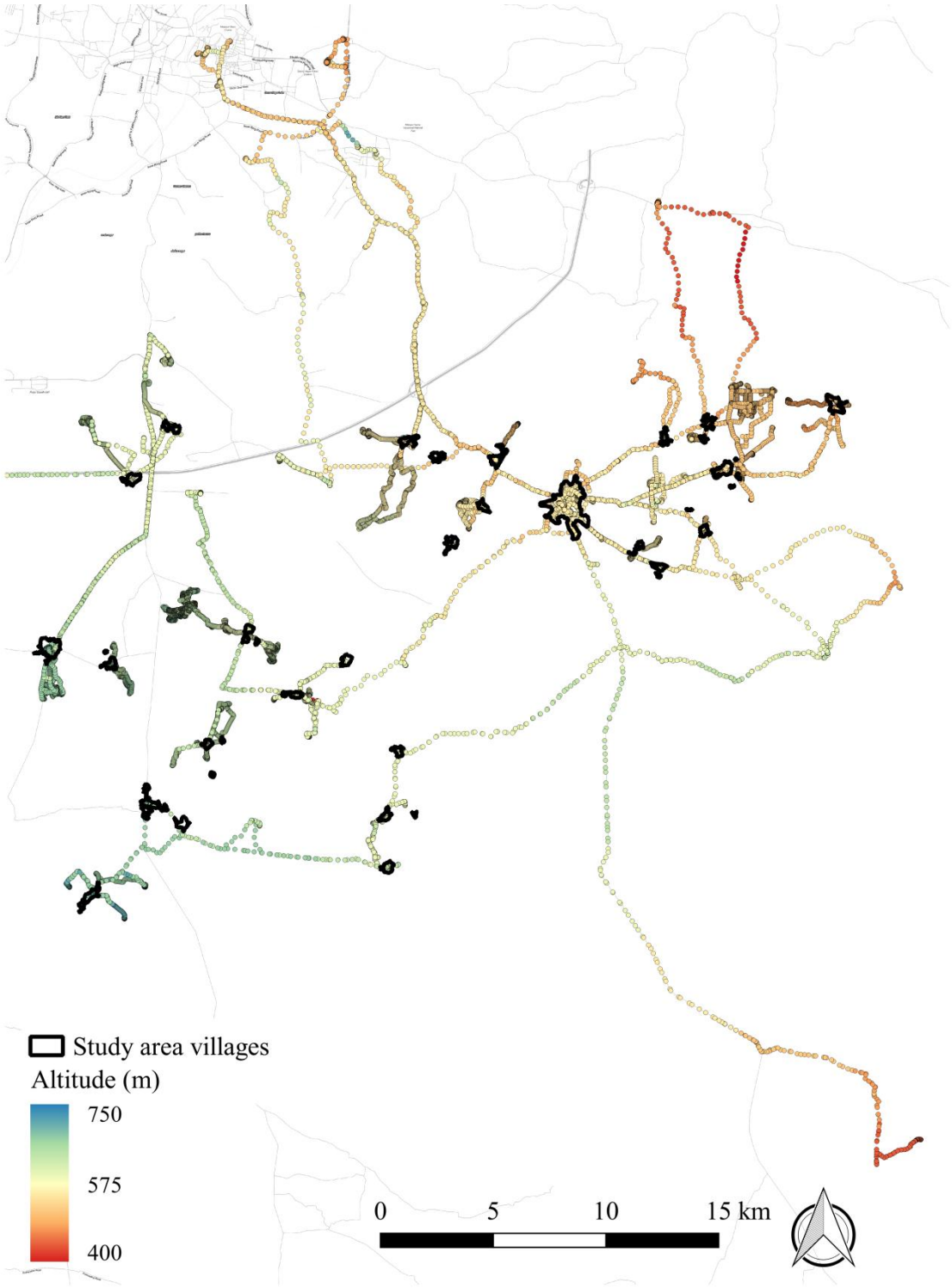

Stamen Toner Lite/OSM used as background map.

Figure S5 Green View Index extraction from a wearable camera photograph example.

Example of a wearable camera picture taken in the study area.

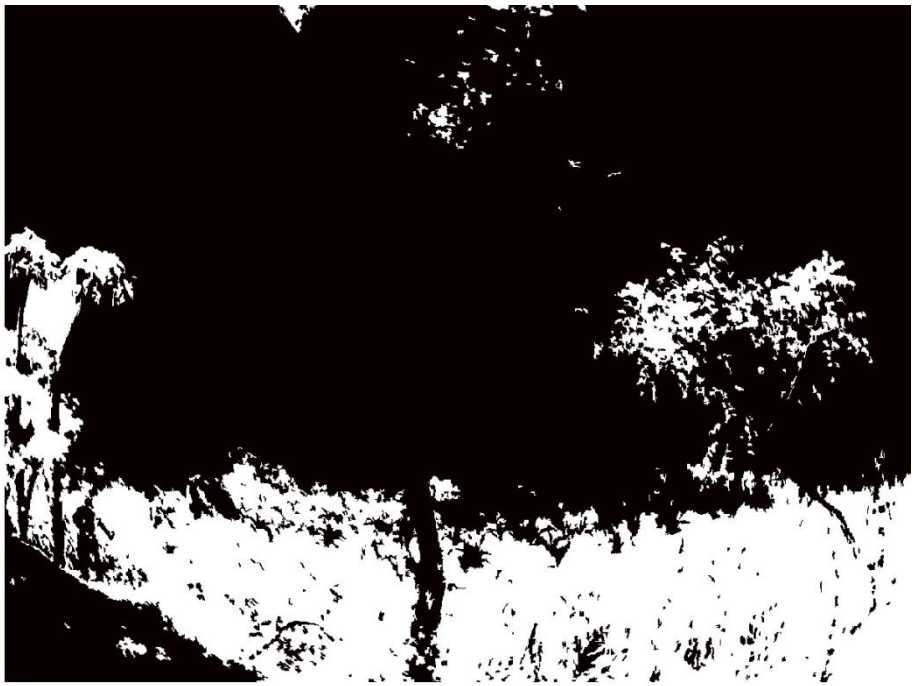

Greenspace (white) extracted from the wearable camera picture. GVI = 24.7%.

Figure S6 Study area NDVI in the summer (A) and post-monsoon (B) seasons.

A)

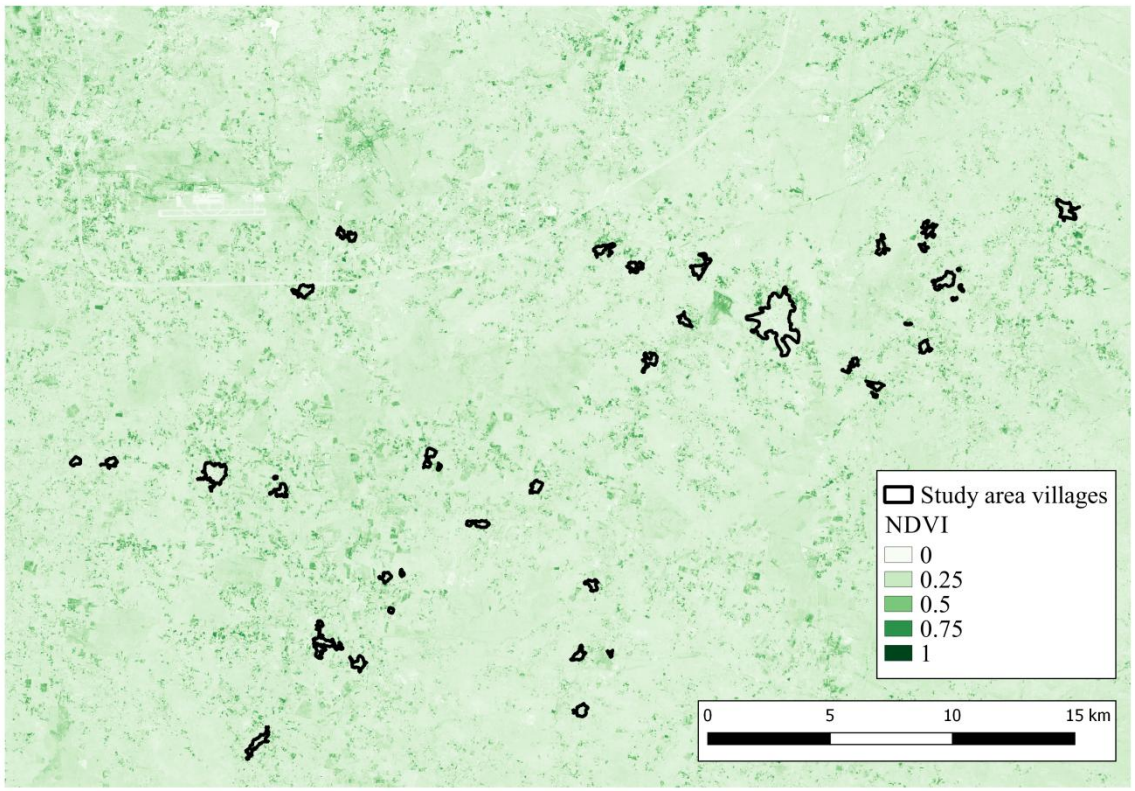

B)

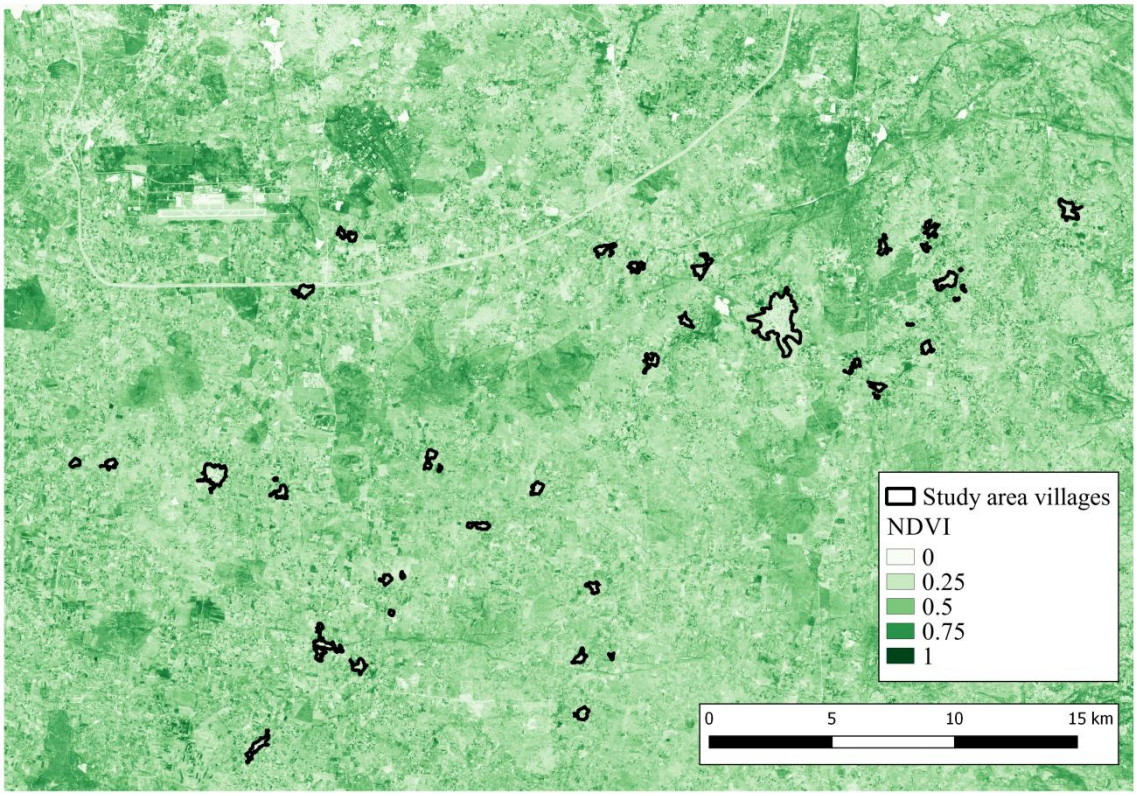

NDVI values smaller than 0 have been coloured as 0 for visualization purposes.

Table S1 Percentage of missing data by dataset and data source.

Data source	Nighttime (N=207)[1]	Daytime (N=227)	Daytime hourly (N=2713)
Personal temperature[2]	2.9%	3.1%	5.6%
Ambient temperature[3]	0%	0%	0%
Baseline questionnaire	0%	0%	0%
Self-reported diary	-	0%	0%
Post-monitoring questionnaire	-	0%	0%
GPS mobility indicators, altitude, and NDVI[2]	0%	8.8%	9.9%
Wearable camera annotations and GVI[4]	-	18.1%	27.5%

[1] Nighttime dataset only included personal and ambient temperature, and self-reported data in the baseline questionnaire. Nighttime GPS indicators were based on geocoded households (whereas daytime's were based on GPS tracks).

[2] Personal temperature and GPS indicators were considered missing when available data for a given time period (nighttime/daytime/ /hour) was lower than 70%.

[3] Ambient temperature previously imputed using data from Hyderabad airport.

[4] Wearable camera indicators were considered missing when available data for a given time period (daytime/nighttime/hour) was lower than 50% (lower threshold motivated by the intermittence of the images).

Methods S2 Data imputation.

We assumed missing completely at random (MCAR) or missing at random (MAR) for data sources included in the different datasets. Missing data was mostly due to device malfunctioning, which we assumed to occur completely at random; and battery exhaustion, which mostly occurred during the last hours of the monitoring. Missing GPS and wearable camera predictors were tracked by similar variables in self-reported diaries (which had no missing data) and were therefore accounted for in the imputation process.

We used multiple imputation to impute the nighttime/daytime/hourly daytime datasets using the method of chained equations implemented in the R package "mice" (van Buuren and Groothuis-Oudshoorn, 2011). We computed 20 imputed datasets for daytime and nighttime datasets, and 30 for the hourly daytime dataset as the proportion of missing data was larger. We imputed personal temperature using linear regression; the rest of predictors were imputed with predictive mean matching. We checked each of the equations and removed predictors highly correlated with each other (e.g., time spent indoors/outdoors). We run the chains for ten iterations, after which a healthy convergence and mixing of the chains was observed. We verified the plausibility of the imputation by comparing the distribution overlap of the observed and the imputed values.

Methods S3 Model selection stepwise procedure.

Even though multiple imputation is one of the most widely used approaches to deal with missing data, there are no clear standards on how to perform model selection in this setting (Schomaker and Heumann, 2014). Our approach was to use a stepwise procedure to select relevant predictors of exposure in nighttime/daytime/hourly daytime datasets that was able to accommodate the imputed data and the repeated measures design. Briefly, starting from a linear mixed model with an intercept only and the corresponding random effects structure, we fitted a model with each of the candidate fixed effects on each of the imputed datasets and combined results using Rubin's rules (Rubin, 2004). For each of them, we tested for variable inclusion using a Wald test (Meng and Rubin, 1992) under the null hypothesis that the coefficient parameter of the included predictor was 0. We chose the variable with the lowest p-value and kept it as a fixed effect in the model for all future steps. We iterated until no candidate fixed effect had a p-value of the Wald test smaller than 0.10. Within each iteration, we tested whether any of the already included variables were no longer significant (Wald test p-value greater than 0.15) and removed it from the model if appropriate. We also checked for collinearity within each iteration (Variance Inflation Factor (VIF) > 5 in 25% of the models fitted on the imputed datasets) and discarded predictors that triggered increases in collinearity (e.g., GPS-intersected NDVI and GPS-100m buffered NDVI). For nighttime/daytime datasets, we used a random intercept per participant in linear mixed models to account for the repeated measures per participant. In daytime hourly analyses, we used a random intercept per monitoring session and used an AR(1) correlation structure to take into account the temporal autocorrelation within session. We could not add an additional random intercept per participant in hourly daytime analyses as some models in the procedure did not converge.

Figure S7 Spearman correlation heatmap of daytime predictors by data source.

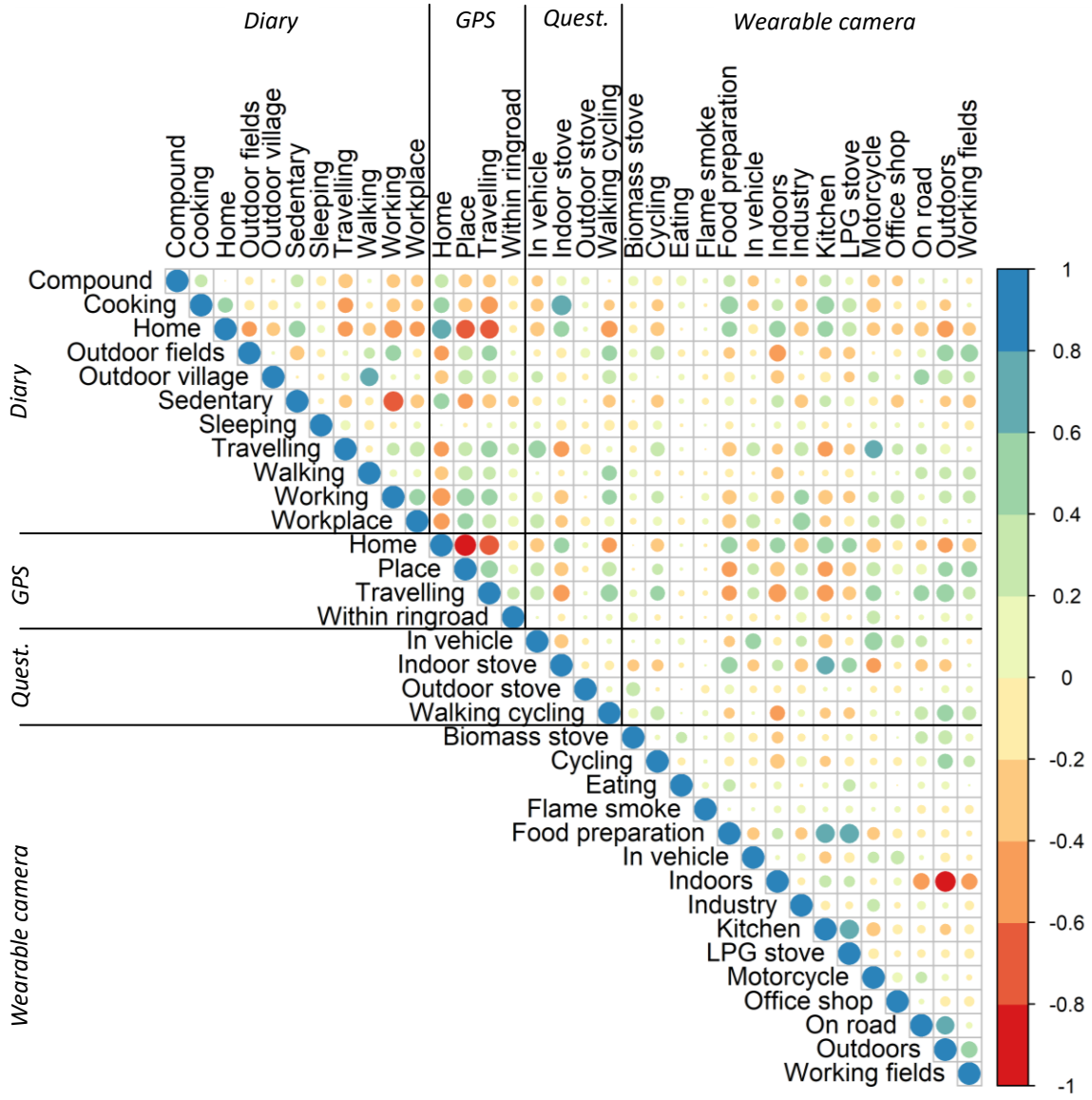

Figure S8 Distribution and association between 1-minute NDVI and GVI.

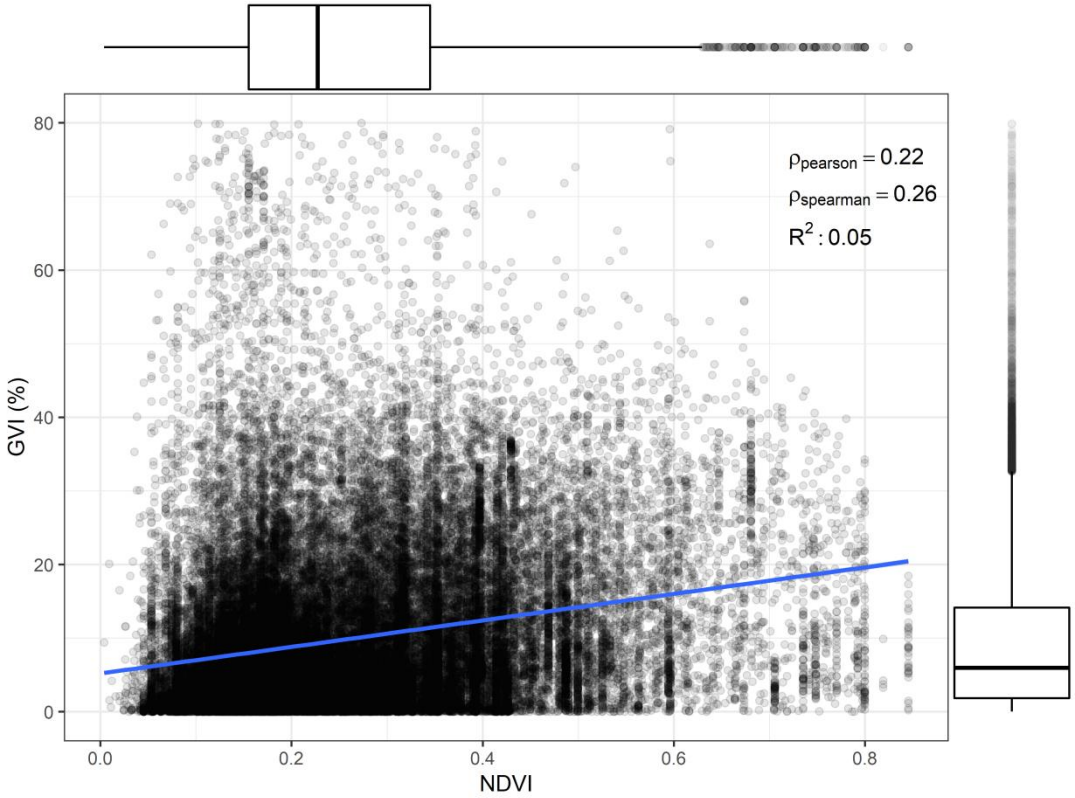

NDVI values smaller than 0 (<0.1%) have been removed for visualization purposes. Only values with collocated NDVI/GVI, i.e., with available GPS track and wearable camera image label as "outdoors", are shown.

Blue line represents linear regression fit of the model GVI ~ NDVI.

In the marginal boxplots, the lower and upper hinges of the box correspond to the 25th and 75th percentiles, the bold bar in the box represents the median. Whiskers are defined as the highest/lowest value within 1.5*Interquartile range from the hinge, values beyond that are plotted as points representing outliers.

Table S2 Ambient and personal summary statistics by season.

Time	Ambient	Personal	Paired differences	p-value
Summer (N=22)				
Daytime	37.6 (3.5)	33.9 (1.9)	3.6 (2.3)	0.000
Nighttime	28.9 (3.5)	31.3 (2.3)	-2.1 (2.7)	0.003
Monsoon (N=96)				
Daytime	30.5 (2.4)	31.7 (2.3)	-1.2 (2.1)	0.000
Nighttime	25.1 (1.6)	29.7 (2.4)	-4.7 (2.2)	0.000
Post-monsoon (N=41)				
Daytime	29.6 (2.4)	30.8 (2.2)	-1.2 (2.1)	0.001
Nighttime	22.7 (1.3)	28.5 (1.9)	-5.8 (2)	0.000
Winter (N=68)				
Daytime	28.3 (2.2)	30.2 (2.6)	-1.9 (2.7)	0.001
Nighttime	19.2 (2.2)	26.9 (2.9)	-7.7 (2.6)	0.000

Temperature expressed as ºC. Summary statistics for ambient, personal, and paired differences correspond to AM (SD). P-value computed with a paired t-test.

Table S3 Gender-stratified predictors of hourly dayttime (6am - 10pm) average personal exposure to temperature.

Temperature predictors (n = 2713)	**Data source**	**Change in ºC (95% CI)**
Women (n = 1398)		
Ambient temperature (1ºC increase)	Ambient fixed site	0.32 (0.28, 0.36)
Asbestos sheets bedroom roof (vs. tiles/grass)	Baseline questionnaire	1.03 (0.06, 2)
Concrete bedroom roof (vs. tiles/grass)	Baseline questionnaire	0.04 (-0.78, 0.86)
Working (1h increase)	Self-reported diary	0.53 (0.18, 0.88)
Altitude (100m increase)	GPS	-0.62 (-1.28, 0.04)
Working in field (1h increase)	Wearable camera	0.83 (0.28, 1.38)
Outdoors (1h increase)	Wearable camera	0.82 (0.47, 1.17)
Men (n = 1315)		
Ambient temperature (1ºC increase)	Ambient fixed site	0.38 (0.34, 0.43)
Asbestos sheets bedroom roof (vs. tiles/grass)	Baseline questionnaire	1.05 (0.03, 2.07)
Concrete bedroom roof (vs. tiles/grass)	Baseline questionnaire	-0.26 (-1.21, 0.68)
Working (1h increase)	Self-reported diary	0.3 (0.03, 0.58)
Altitude (100m increase)	GPS	-0.99 (-1.63, -0.36)
Travelling (1h increase)	GPS	0.78 (0.43, 1.13)
Outdoors (1h increase)	Wearable camera	0.61 (0.24, 0.98)

Gender-stratified linear mixed model (random intercept per session, AR(1) correlation structure) models fit to multiply imputed datasets and pooled using Rubin's rules.

References

Meng, X.-L., Rubin, D.B., 1992. Performing Likelihood Ratio Tests with Multiply-Imputed Data Sets. Biometrika 79, 103–111.

Rubin, D.B., 2004. Multiple imputation for nonresponse in surveys. John Wiley & Sons.

Schomaker, M., Heumann, C., 2014. Model selection and model averaging after multiple imputation. Comput. Stat. Data Anal. 71, 758–770. https://doi.org/10.1016/j.csda.2013.02.017

van Buuren, S., Groothuis-Oudshoorn, K., 2011. mice: Multivariate Imputation by Chained Equations in R. J. Stat. Softw. 45, 1–67.